CHALMERS

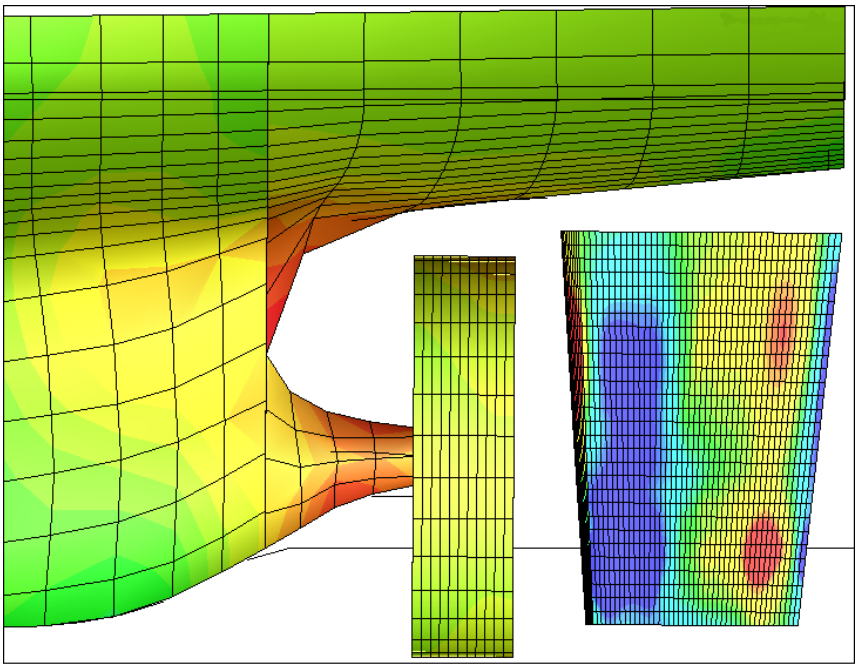

Investigation of propeller characteristics with different locations of the rudder

Master of Science Thesis

ARASH JAMALI

Department of Shipping and Marine Technology
Division of Sustainable Ship Propulsion
CHALMERS UNIVERSITY OF TECHNOLOGY
Göteborg, Sweden, 2010
Report No. X-10/253

A THESIS FOR THE DEGREE OF MASTER OF SCIENCE

Investigation of propeller characteristics with different locations of the rudder

ARASH JAMALI

Department of Shipping and Marine Technology
CHALMERS UNIVERSITY OF TECHNOLOGY
Göteborg, Sweden 2010

Investigation of propeller characteristics with different locations of the rudder

ARASH JAMALI

Report No. X-10/253

Department of Shipping and Marine Technology
Chalmers University of Technology
SE-412 96 Göteborg
Sweden
Telephone +46 (0)31-772 1000

Printed by Chalmers Reproservice
Göteborg, Sweden, 2010

Investigation of propeller characteristics with different locations of the rudder

ARASH JAMALI
Department of Shipping and Marine Technology
Chalmers University of Technology

Abstract

In designing a ship, propulsive efficiency is a parameter which always is tried to be kept as optimum as possible. An investigation in full scale and model scale of a ship including propeller and rudder, regarding the effect of changing rudder position on variation of propeller characteristics has been carried out. SHIPFLOW software was utilized to apply Computational Fluid Dynamic (CFD) techniques in order to compute the flow around the ship hull, propeller and rudder. Lifting line method which is coupled with RANS solver module of SHIPFLOW is used to simulate and also compute the propeller characteristics. Five different longitudinal rudder positions were investigated and compared to each other in order to determine the optimum longitudinal position of rudder. Furthermore, in model scale, for optimum longitudinal rudder position, one different transverse position of rudder was also evaluated. For computing propeller characteristics, SELFPROPULSION command was applied into computations in order to achieve balance between drag and thrust by adjusting the shaft RPM.

In order to evaluate the accuracy of results for these two different scales, computed results for original rudder position in model scale and full scale were compared with test results and predicted results by ITTC 1978 method, respectively. Computed results in model scale, thrust and torque, show a good agreement with test results but obtained results from computations for full scale, such as delivered power and effective power seem to be over predicted compared to predicted results by ITTC 1978 method.

Consequently, optimum rudder position was determined based on model scale results which are reasonably accurate compared to full scale computed results. The reason which made full scale computation results over predicted can be described regarding to grid resolution at the aft part of ship hull which is not compatible with propeller grids. This causes inaccurate interpolation between propeller and hull/rudder grids which concludes over predicted results for full scale.

Keywords: Propeller characteristics; lifting line; SHIPFLOW; selfpropulsion; ITTC 1978 method; grid resolution; optimum rudder position.

Preface

This thesis has been done to complete the Master program of Naval Architecture at Chalmers University of Technology. The study has been accomplished at Chalmers University of Technology, Department of Shipping and Marine Technology, Göteborg with cooperation of Rolls-Royce Hydrodynamic Research Centre and Wallenius Marine AB.

Hereby, I would like to show my appreciation to my examiner, Professor Rickard Bensow, my supervisor Göran Grunditz from Rolls-Royce Company, Björn Regnström from FLOWTECH, Martin Edmark from ANSYS Company and PhD students, Arash, Martin Daniel and Florien.

I would like to thank my family and my aunt who always have been supporting me by their kindness. I also would like to thank my classmates, Johannes, Mostafa, Mark, and Ozan who made unforgettable memories for me during doing my master thesis at university.

Göteborg, December, 2010
Arash Jamali

Contents

1. Introduction

Regarding the environmental concern and increase of fuel price, optimizing the fuel consumption is nowadays an important issue in all industries. In ship industry one way to decrease the fuel consumption is improving the propulsion system of the ship which results higher propulsive efficiency.

One of the options to reach this aim is evaluation of different locations of the rudder in order to improve the propulsive efficiency. It would be time consuming and not cost effective to make a model of every rudder location. Computational fluid dynamic is a good solution for this problem, because you can easily do several cost effective test in a proper amount of time. Different rudder positions can be modelled and simulated in order to improve and optimize the design by trying to increase the propulsion efficiency and at the same time decreasing the side effects such as cavitation and loss in manoeuvrability.

1.1. Background

Rolls-Royce Hydrodynamic Research Centre located at Kristinehamn is interested in evaluating the interaction of rudder and propeller in different longitudinal position of the rudder behind the working propeller. The thesis input data is including geometry and operating conditions of ship hull, rudder and propeller, was supported by Wallenius Marine AB. The thesis was done at the department of Shipping and Marine Technology at Chalmers University of Technology. Instead of building models and testing them in towing tank or cavitation tunnels, it was preferred to do this evaluation by help of CFD technique which is a cheaper way compared to making models. SHIPFLOW software is chosen as a CFD tool which is very applicable in marine industry.

1.2. Objective

The existing work is concentrated on study of hull/propeller/rudder interaction by numerical methods to investigate fluctuation and find the optimum results of calculated propeller operating point, delivered power, thrust and total resistance for different rudder positions behind working propeller. Computations will be performed for both full scale and model scale to see the scale effect on optimum rudder position from propulsive characteristics point of view. Furthermore, an investigation will be done to evaluate the accuracy of CFD computations by comparing the CFD results of model scale and full scale respectively with data obtained from experiments which were done on ship model and predicted data for full scale.

1.3. Methodology

Ship hull was given as a rough offset file from Wallenius Marine AB, representing a typical Ro-Ro vessel. That offset file could be imported to SHIPFLOW software as an output but in order to make a better mesh on the ship hull, first of all an IGES file of ship hull body was created by that given offset file in RHINOCEROS software, then that IGES file was imported into SHIPFLOW in order to make finer offsets of hull.

For computing wave pattern and wave resistance, potential flow method has been used. Furthermore, the free surface effect is also applied in potential flow calculation which is maintained fix for the rest of computation procedure. The result of potential flow computation is used as an input data for boundary layer method computation. Boundary layer method calculates the flow parameter in half forward of the ship hull.

RANS equation is solved for turbulent flow in aft part of the ship. Body forces are calculated by modelling the propeller as an actuator disc which operates in effective wake field. For analyzing different rudder locations and their interactions and effects on propeller performance, Lifting line method which is coupled with SHIPFLOW RANS solver XCHAP is chosen.

It is preferred to import the rudder as an external mesh. External mesh which is including schilling rudder mesh and domain around the rudder mesh is created in a mesh making software. Then generated grids are imported to SHIPFLOW. Propeller performance parameters such as flow field, thrust, torque and resistance in different positions of rudder from propeller are computed with help of SHIPFLOW. In the next step computed parameters for all different rudder positions are compared to each other in order to determine the optimum rudder position.

2. Theory

In this part a short description will be given about the propeller/rudder interaction, Schilling rudder, SHIPFLOW software and Lifting line method for analysing the propeller characteristics.

2.1. Propeller theory

To propel ships, a propulsor which can be called propeller is needed. The aim is to create required thrust T for moving ship at a specific speed V and overcoming the resistance R_T which is applied from water to the ship body.

Propeller diameter plays an important role in increasing propulsive efficiency. The bigger possible propeller diameter, the higher propulsive efficiency is approachable [8]. However, there are some limitations which effect on the size of propeller diameter. For example, shape of the aft part of the ship hull is really important where the clearance between the propeller tip and hull should be considered.

Ballast condition is also important depending on type of ships. Tankers and bulk carriers for example whose propellers run in fully immersed condition, size of propeller is limited regarding to the minimum water depth of working area. Furthermore, it can be mentioned that usually propellers with large diameter do not rotate fast.

Number of propeller blades is another issue in designing and selecting propeller for a ship. Considering conditions that are supposed to be fulfilled, propellers are designed with 2, 3, 4, 5 and even 6 blades. About the propeller efficiency, according to the propeller blade number point of view, it can be mentioned that, the less number of blades, the higher propeller efficiency is achievable. However it should be kept in mind that when the propeller is subjected to high loads, considering the strength of propeller, number of blades is usually more than 2 or 3.

Figure 1 shows more details of propeller geometry with important related parameters. Some of them are mentioned in following:

- Propeller Blade (2)
- Propeller Hub (3)
- Leading Edge (20)
- Trailing Edge(21)
- Expanded Blade Area (25)
- Propeller Radius (31)
- Leading Edge Length (32)
- Trailing Edge Length (33)
- Profile Thickness (34)
- Profile Camber (35)
- Pitch Angle (40)
- Pitch (41)

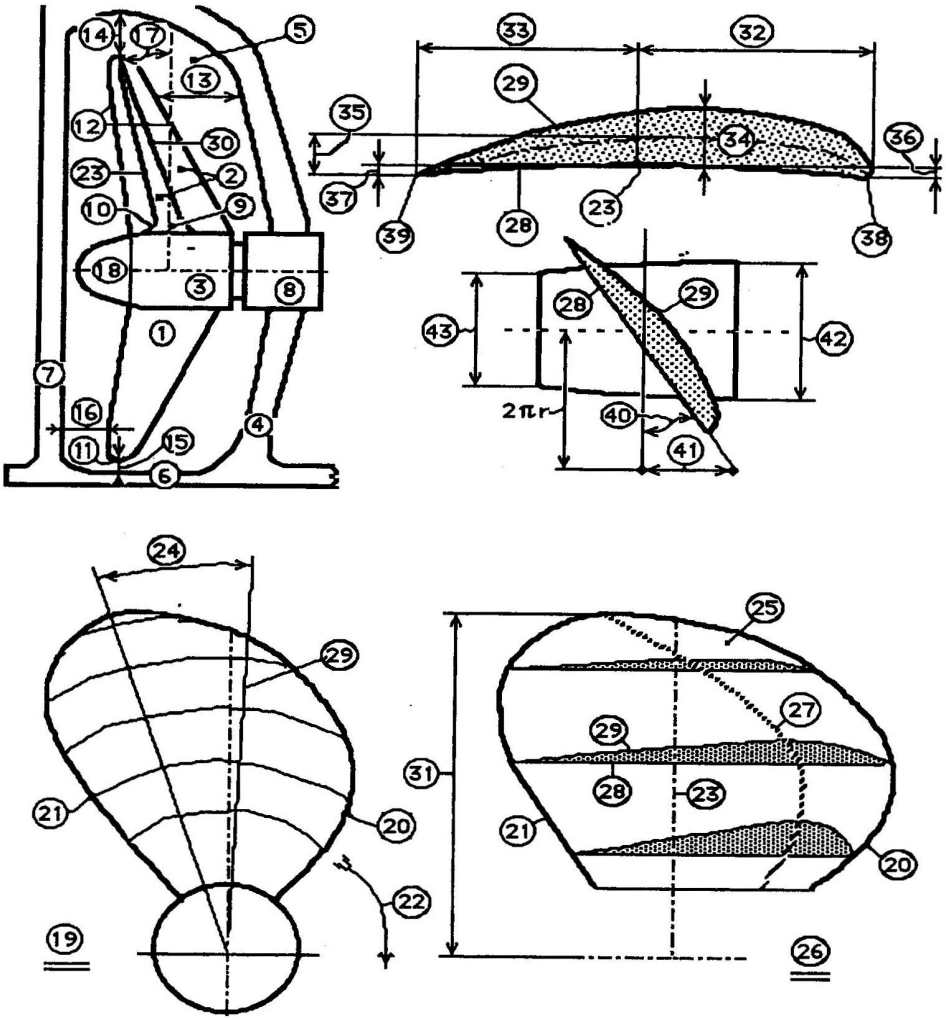

Figure 1. source:[1]

In designing propellers some defined parameters play an important role and are called propeller characteristics. Typical propeller characteristics are advance coefficient J, thrust coefficient $K_t$and torque coefficient K_q. The definitions of these parameters are:

$$J = \frac{\mathrm{V_A}}{\mathrm{nD}} \quad (1)$$

$$K_t = \frac{\mathrm{T}}{\rho \mathrm{n^2 D^4}} \quad (2)$$

$$K_q = \frac{\mathrm{Q}}{\rho \mathrm{n^2 D^5}} \quad (3)$$

The generated power P_D by engine, is delivered to the propeller and calculated by equation 4

$$P_D = 2\pi n Q_n \quad (4)$$

V_A is advance velocity, T is the thrust and Q_n is the generated torque by the propeller and D is propeller diameter.

The open water efficiency η_0 is the efficiency of propeller working in a homogeneous flow without any ship hull. It is defined as thrust power P_T divided by P_D which is the shaft power.

$$\eta_0 = \frac{T V_A}{P_D} = \frac{J K_T}{2\pi K_Q} \quad (5)$$

Propulsive efficiency $\eta_D$which should not get mixed up with open water efficiency η_0, is equal to effective power P_E divided to shaft power P_D.

$$P_E = R_{TS} V_s \quad (6)$$
$$P_D = 2\pi n_S Q_s \quad (7)$$
$$\eta_D = \frac{P_E}{P_D} \quad (8)$$

In these equations, R_{TS} is total ship resistance, V_s is ship speed, n_s and Q_s are shaft revolution rate and applied torque to the shaft respectively [1].

By towing a ship hull, at the stern a high-pressure region is observed which affects the total resistance of the ship. During the self propulsion test, high-pressure area located at the aft part of the ship is affected by a working propeller. Therefore magnitude of pressure in this high-pressure region is reduced. Consequently, there is an increase in resistance due to existence of propeller. For propelling the ship at a specific speed V_S, produced thrust T by the propeller should be larger than total resistance of the ship hull R_T. Thrust deduction t is the normalized form of difference between T and R_T and is defined as in equation (9).

$$t = \frac{T - R_T}{T} = 1 - \frac{R_T}{T} \quad (9)$$

Because of the friction wake at the aft part of the ship where the propeller is working, the velocity of water V_W at the propeller plane is less than the speed V of the ship. The direction of V_W is in the same direction of ship movement. Meanwhile, the propeller is accelerating the water flow with the speed of V_A in the opposite direction of the ship's speed.

V_W is called effective wake velocity at the propeller which is obtained by subtracting ship's speed V from propeller advance velocity V_A.

$$V_W = V - V_A \quad (10)$$

Wake fraction is a dimensionless form of effective wake velocity and is defined as:

$$W = \frac{V_W}{V} = \frac{(V - V_A)}{V} \quad (11)$$

Some factors such as shape of ship hull, size and position of propeller, affect the wake fraction and therefore the propeller efficiency. Figure 2 gives more description about the parameters related to propulsion of a ship.

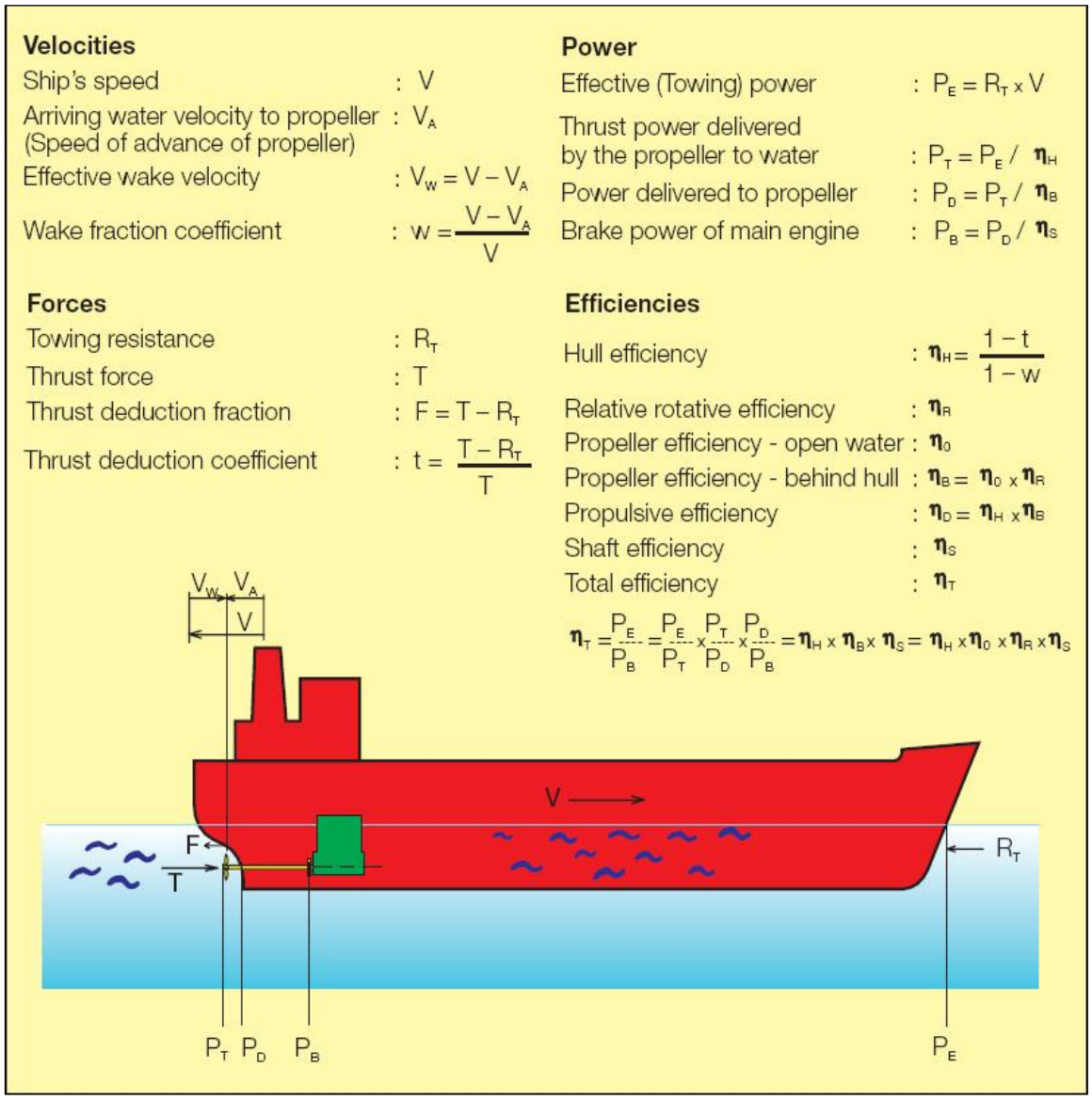

Figure 2. Some relevant definitions of velocity, force, power and efficiency parameters of ship, source: www.manbw.com/files/news/filesof3859/P254-04-04.pdf

2.2. Propeller/rudder interaction

For approaching better manoeuvrability in ships, rudders are installed behind the propellers where they are faced by high-energy propeller slipstreams. These slipstreams contain axial and tangential induced velocity created by the propeller. The flow properties and hydrodynamic performance are different when either rudder or propeller is working alone in aft part of the ship hull. A rudder which is situated in these high-energy slipstreams is facing different axial forces such as:

- Tangential velocity induced by propeller applies a thrust force on the rudder. In addition it can be mentioned that, the rudder recovers rotational energy of rotational slipstreams caused by the propeller. This recovery happens when the rudder also induces tangential velocity in opposite direction of the propeller slipstreams flow which cancel out a fraction of propeller induced tangential velocity.

- Due to induced axial velocity by the propeller in onset flow, the viscous drag force on the rudder is increased.
- The flow which has been accelerated by the propeller increases the pressure drag on the rudder.

Furthermore, as it is shown in Figure 3, the streams coming out of the propeller get blocked and diverted by the rudder which results in decreasing the total axial and tangential velocity. Thrust and torque will therefore be partly higher when a rudder is included. Consequently higher propulsive efficiency might be obtained from propeller/rudder combination as a propulsion system [2].

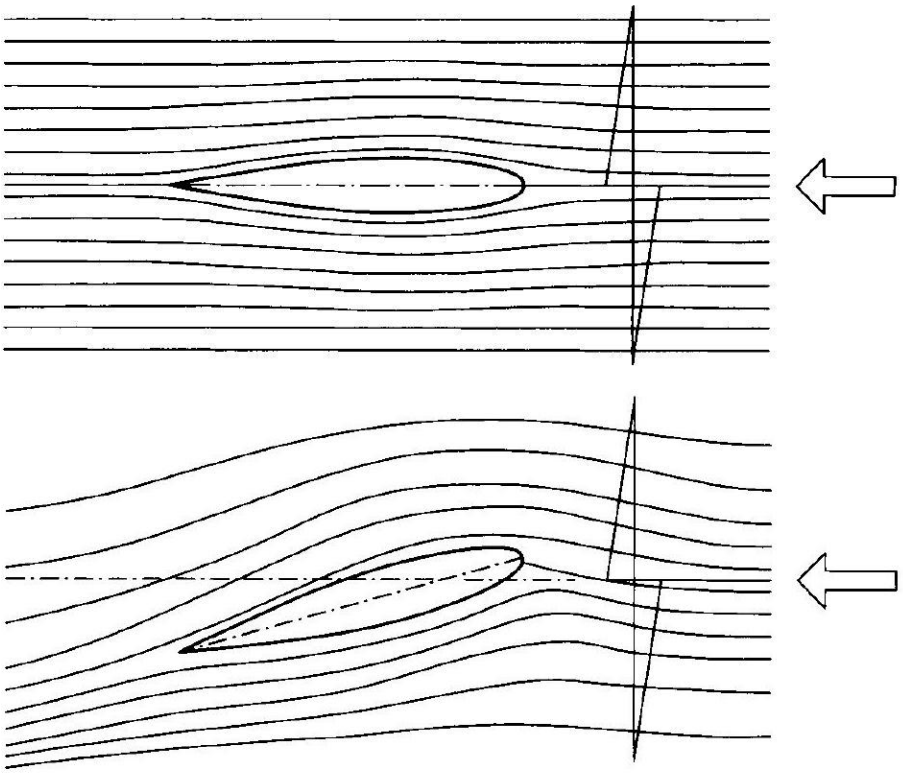

Figure 3. Blocked and diverted flow by rudder

2.2.1. The Schilling rudder

The idea behind the Schilling rudder design is to use the propeller slipstreams efficiently. A better manoeuvrability is achieved by this type of rudder regarding its capability of turning 70° in port and starboard direction. For conventional rudders this turning angle is half of the Schilling rudder.

Schilling rudder which has fish body shape horizontal cross section is made as one piece construction. Since no moveable parts are included, the need for maintenance is low. Furthermore about the Schilling rudder, it can be mentioned that the course quality is stable and good. In addition, light weight and low cost can be counted as other advantages of this type of rudder. As it is shown in Figure 4, blunt leading edge and fishtail trailing edge are effective to have good flow properties which help to recover the lift at the trailing edge.

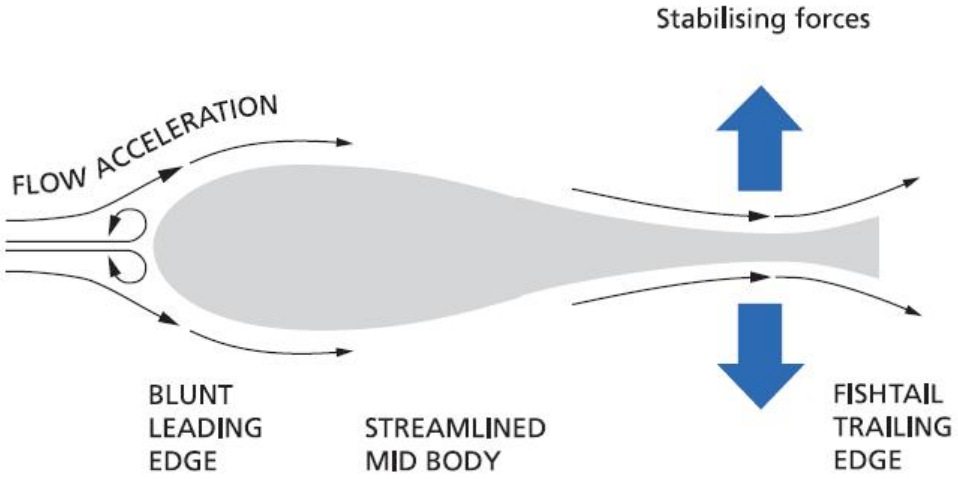

Figure 4. Schilling rudder cross section**,** source: www.becker-marine-systems.com

2.3. SHIPFLOW

In this part a brief description will be given about abilities and strength of SHIPFLOW which is used in this study as a CFD software to analyze the flow around ship hull, propeller and rudder.

2.3.1. Different approaches (zonal and global)

SHIPFLOW is a CFD software which is developed by FLOWTECH international AB. With the help of this software, flow around the ship hull can be predicted and analyzed. In order to analyze the flow around the hull, two approaches have been designed in this software. These approaches are Global approach and zonal approach. In this study, zonal approach has been executed to compute the flow characteristic around the ship hull and propulsion parameters of the propeller.

In zonal approach, flow around the hull as shown in Figure 5 is divided into three zones. In zone 1, in farthest out of the region around the hull, potential method is executed. The fluid flow in this area is irrotational and inviscid. In order to calculate the fluid flow parameters in boundary layer along the ship hull which is shown as zone 2, boundary layer method is used. The input for executing this method is provided from potential flow calculation results. The flow in aft part the ship hull, zone 3 will be turbulent and viscous effects are not negligible. RANS (Reynolds-Averaged Navier-Stokes) is executed to compute the flow characteristics in this area.

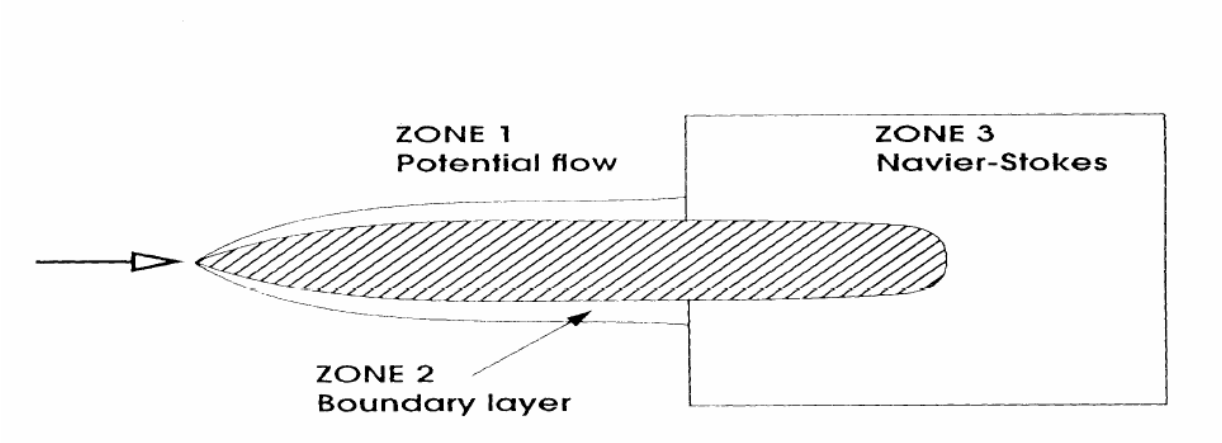

Figure 5. Zonal approach

2.3.2. Overlapping grids

SHIPFLOW has the ability to handle the overlapping grids which are used for analyzing the flow around complex geometries. Furthermore, even though SHIPFLOW is able to create overlapping grids for appendages, in some cases it is difficult to create the exact shape of the required geometry. Another strong point about SHIPFLOW is used which is the ability of importing overlapping grids. In order to locate the imported grids in adequate positions, it is possible to move, rotate and even resize the grids.

Different boundary conditions such as noslip, slip, inflow, outflow, interior and inout can be defined for imported grids regarding the boundary of fluid domain around the grids surfaces [5].

2.3.3. SHIPFLOW Modules

Modules in SHIPFLOW which are categorized to five parts are:

XMESH

XMESH is a grid generator module which creates mesh for potential flow method calculation. It has the ability to run separately in order to check the panelization of the body and the free surface.

XPAN

XPAN is the potential flow solver module in SHIPFLOW which computes the flow around 3D objects by using surface singularity panel method. The characteristics which can be computed by XPAN are:

- Wave resistance from pressure integration and from transverse wave cuts
- Wave pattern
- Wave profile along the waterline
- Wave profile along longitudinal and transverse wave cuts
- Far-field waves in deep water
- Potential streamlines (traced in XBOUND)

- Pressure contours
- Velocity vectors
- Sinkage and trim
- Lift and induced drag

XBOUND

XBOUND module is executed to compute the flow in thin turbulent boundary layer by solving the momentum integral equation. This module is also able to compute the laminar and transition boundary layers. The parameters that are computed by XBOUND are:

- Boundary layer thickness
- Displacement thickness
- Momentum thickness
- Shape factor
- Cross-flow angle
- Skin friction coefficient
- Transition between laminar and turbulent flow
- Limiting streamlines

XGRID

XGRID generates grids for computing the turbulent flow which is obtained by solving RANS equations.

XCHAP

XCHAP is executed to solve the RANS equations based on finite volume code. This module which can be applied in zonal and global approach uses different turbulent models such as EASM, k-w BSL and k-w SST. When the zonal approach is used, the boundary condition values for executing XCHAP module are taken from XPAN and XBOUND computation results. Parameters which are computed by XCHAP are:

- Velocity field
- Pressure
- Turbulent kinetic energy and specific turbulent kinetic energy.
- Local skin friction coefficient
- Friction and pressure resistance coefficients for the hull part covered by the grid
- Total resistance and its components using the results from XPAN, XBOUND and XCHAP

XCHAP can also be executed on imported structured grids to SHPFLOW [3].

2.4. Lifting line method for analyzing the propeller

Lifting line is a method to calculate the propellers characteristics which was proposed by H. W. Lerbs in 1952. In this method a propeller with finite number of blade, B, blade is modelled

with a vortex system including hub vortex, bound vortex and helical free vortex. The vortex system is created as: hub vortex is generated along the X axis, B bound vortex lines are generated corresponding every blade and B helical free trailing vortex line tracing the propeller slipstream at specific radius. This vortex system is shown in Figure 6 and Figure 7. Induced velocity by the propeller is divided into two different parts regarding the time dependency point of view. The steady part forms the major part of the induced flow which is not dependent to the time, and the time dependent part. An infinite-bladed propeller is utilized, in order to simplify the estimation of time independent part of the induced flow. In the case of the infinite-bladed propeller, the vortex system is applied by executing a sequence of bound vortex and helical vortex lines which are distributed between the propeller hub with the radius R_{HUB} and propeller tip with the radius R. An assumption about helical vortexes is made which implies that the radius and pitch of all helical vortices are constant in the axial direction [5], [2].

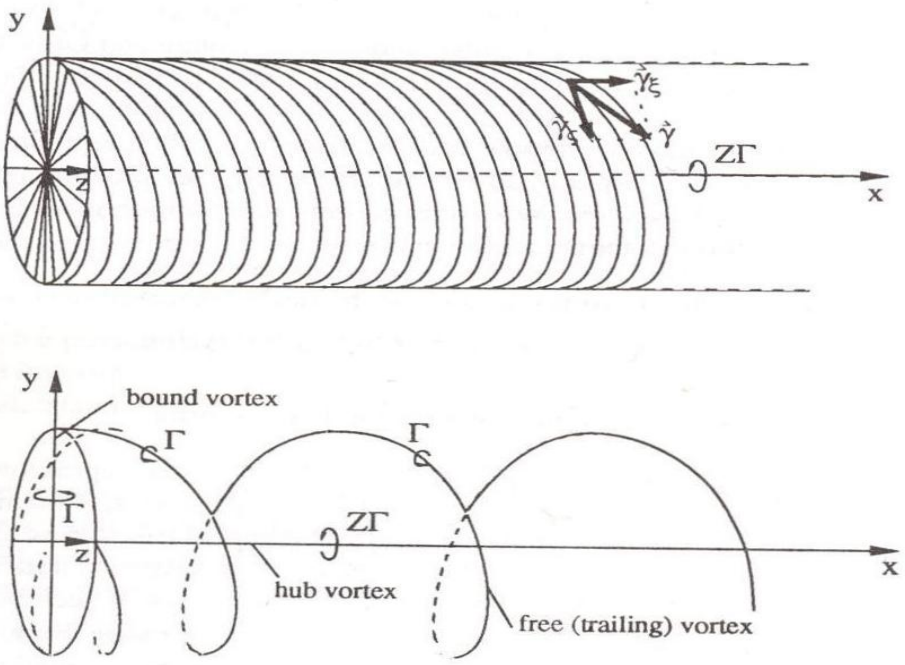

Figure 6. Lifting line vortex system of propeller with infinite number of blade (upper image) and Z blade number (lower image). Source: [2]

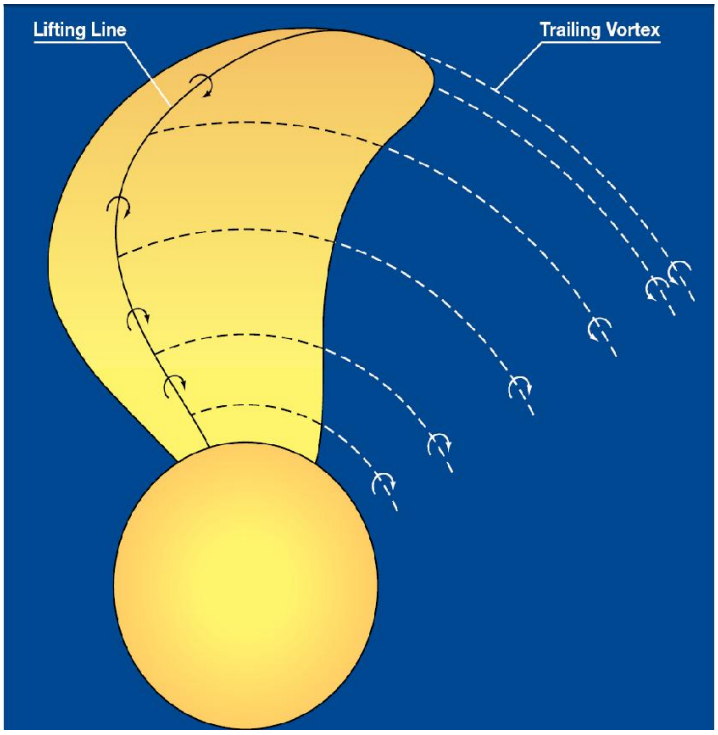

Figure 7. Lifting line vortex system of propeller, source: www.manbw.com/files/news/filesof1815/Hydrod%20propellers.pdf

In SHIPFLOW software, lifting line method is coupled with XCHAP solver in which the propeller is modelled as infinite-bladed propeller.

3. Geometry, Mesh and Work Procedure

3.1. Geometry

Computations in this study are applied on a set of three different geometries. These geometries are, a Ro-Ro ship hull, a FP propeller and a Schilling rudder.

Table 1. Main particulars of the ship

Length LPP [m]	190
Length LWL [m]	223
Draft [m]	10
Beam [m]	32.26

Approximate ship hull geometry data was given by Wallenius Marine AB and represents a typical Ro-Ro vessel. In order to get a good quality of generated mesh, additional offset lines have to be created along the ship hull length. Also increasing the density of offsets in fore and aft part of the ship will help to create higher quality mesh for these curvature shape areas. To reach this aim, an IGES file of ship geometry which is seen in Figure 8 was created by importing the existing offset file of ship hull into RHINO software. A higher quality offset file was made out of this IGES file by help of SHIPFLOW. Some data about ship hull geometry is shown in Table 1.

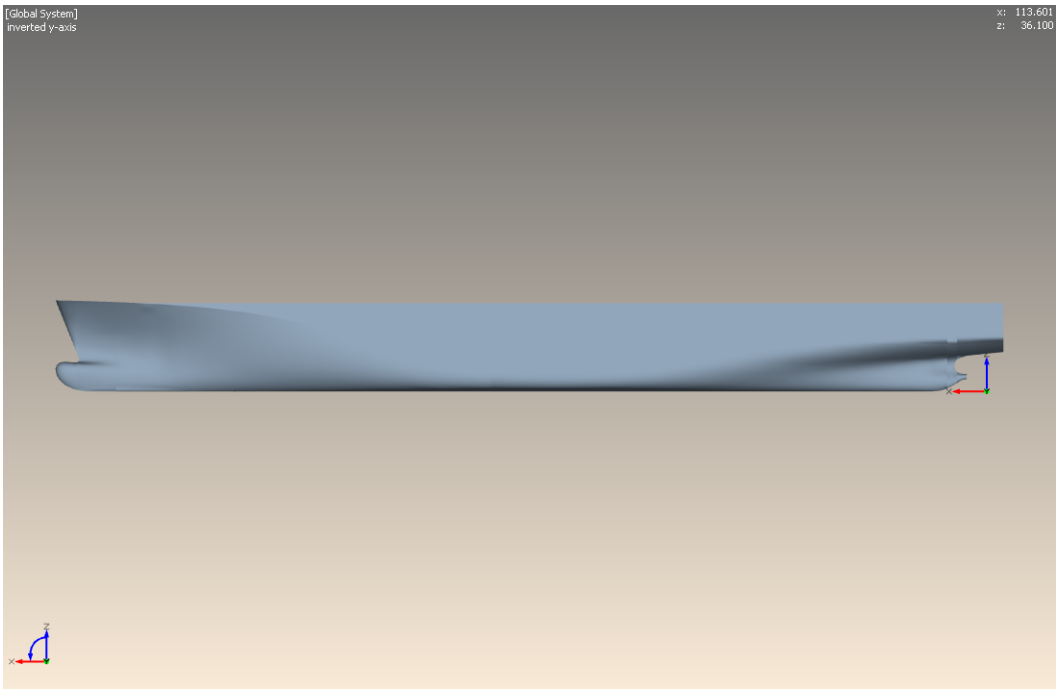

Figure 8. Created ship hull out of primary offset lines

Propeller geometry and its position are specified by a command. The propeller is modelled as an actuator disk in CFD simulation by SHIPFLOW software. Some propeller data is shown in Table 2.

Table 2. Some of the propeller's data

Propeller diameter	6800 mm
Hub diameter	1020 mm
Number of blades	4
Rate of revolution	110 rpm

Schilling rudder geometry which is seen in Figure 9 was received as an IGES file. Then a domain was created around the rudder by RHINO software and finally rudder and domain grids were imported as an external mesh into SHIPFLOW for computations.

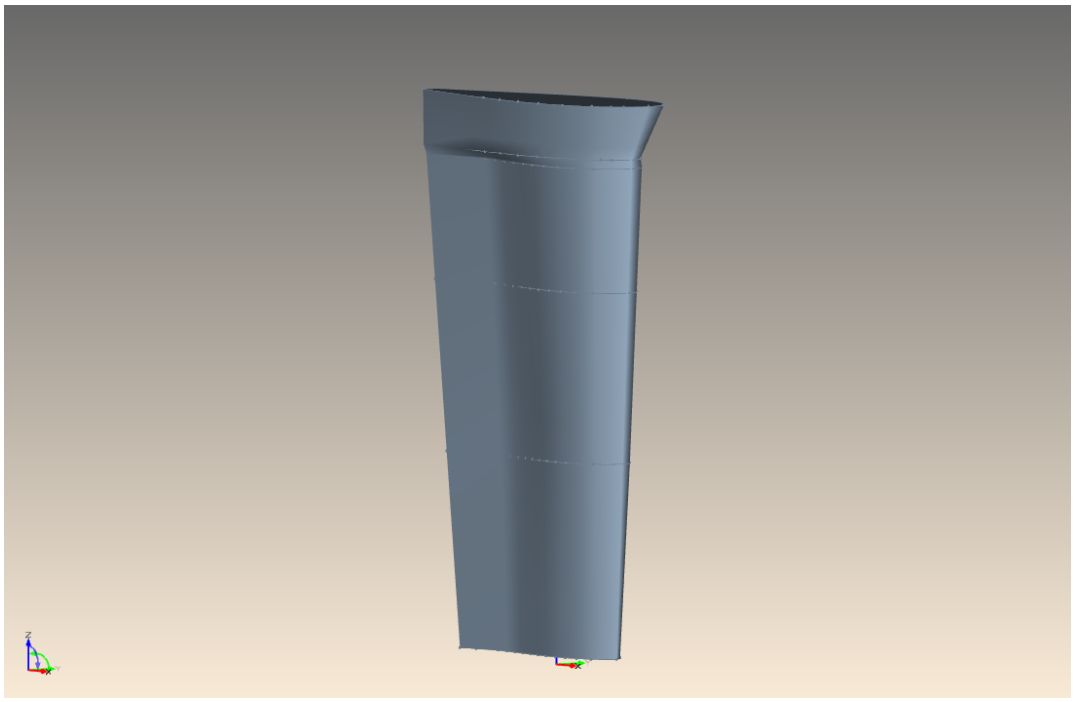

Figure 9. Schilling rudder geometry

3.2. Grids

In this project, grids were made in two different software. Mesh on the ship hull, free surface and propeller were made in SHIPFLOW. As mentioned before for potential flow calculations, required mesh was generated by XMESH module and for RANS calculations, grids were created by XGRID module. Figure 10 shows generated mesh on ship hull body and free surface.

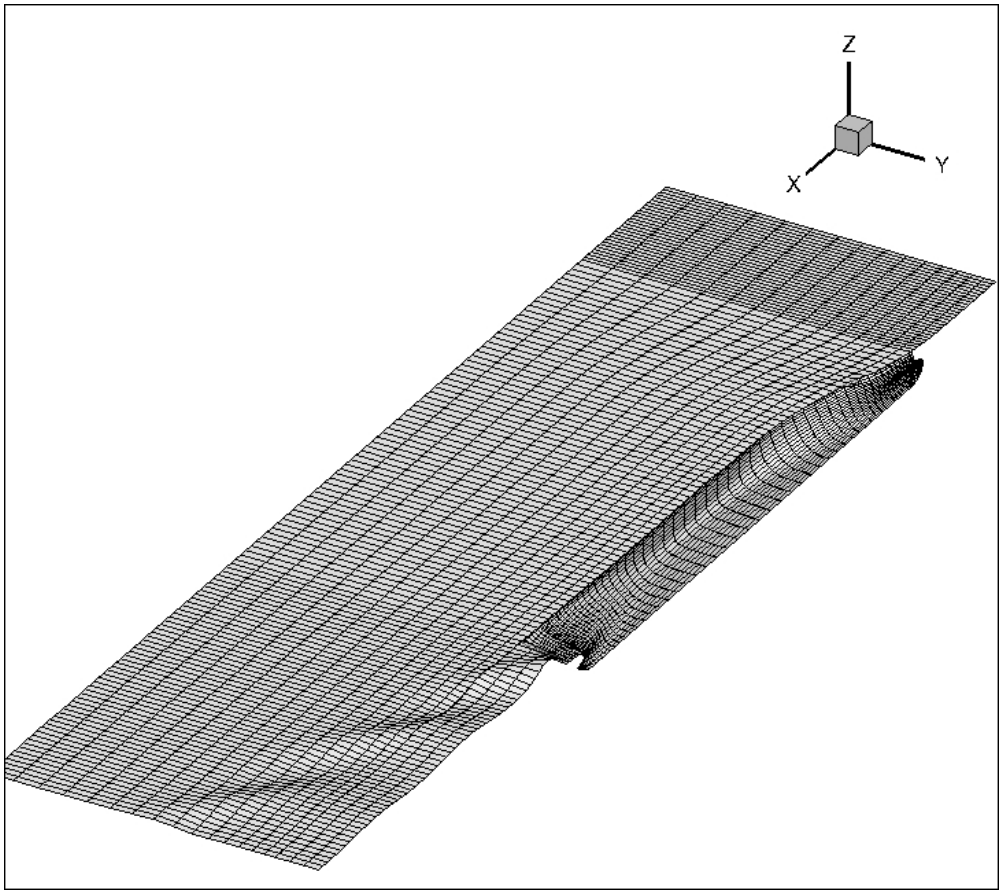

Figure 10. Generated mesh on ship hull body and free surface.

SHIPFLOW has the ability to model the rudder geometry by writing a specific command by which the rudder geometry data is imported into the computations. In order to have the exact rudder geometry it was preferred to make the mesh on the rudder by mesh generator software and then the created rudder mesh was imported into SHIPFLOW as an external mesh. The imported grid should be structured and in Plot3D format file. The rudder/domain mesh was created in GAMBIT software. GAMBIT is not able to export the mesh in Plot3D format, therefore GAMBIT mesh was translated to Plot3D format in ANSYS ICEM CFD software.

Figure 11 shows generated mesh on rudder and domain around the rudder created in ANSYS ICEM CFD software. Overlapping grids which are rudder girds with ship hull/propeller grids can be seen in Figure 12.

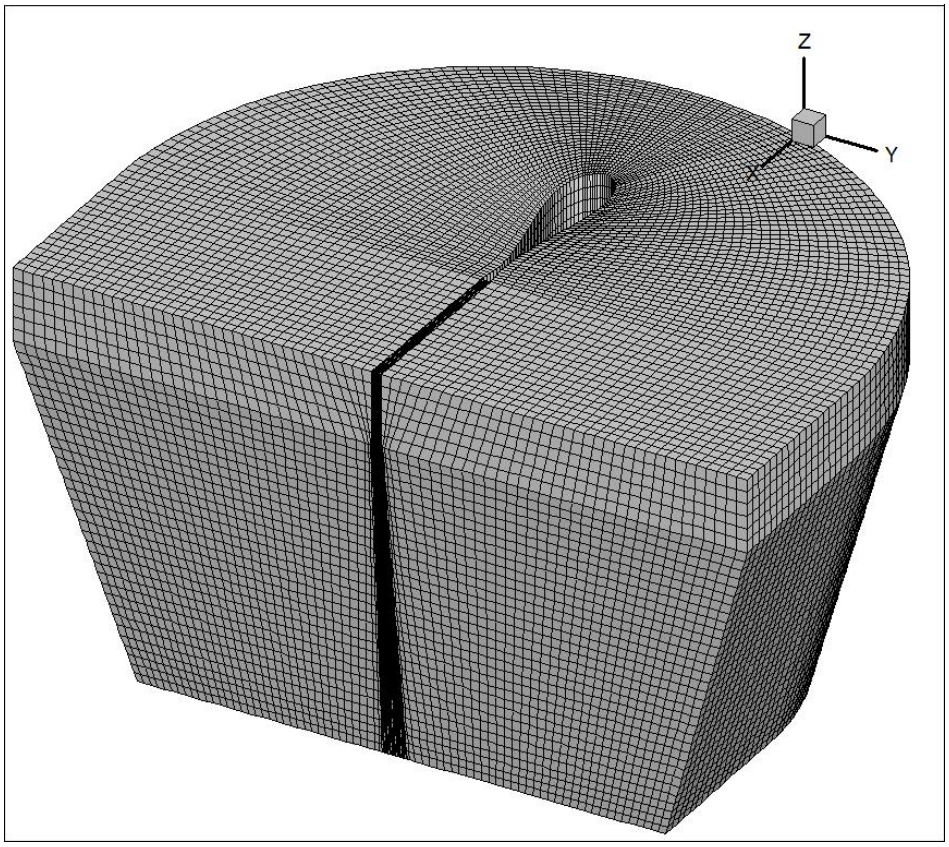

Figure 11. Grids of rudder and domain around the rudder in Plot3D format

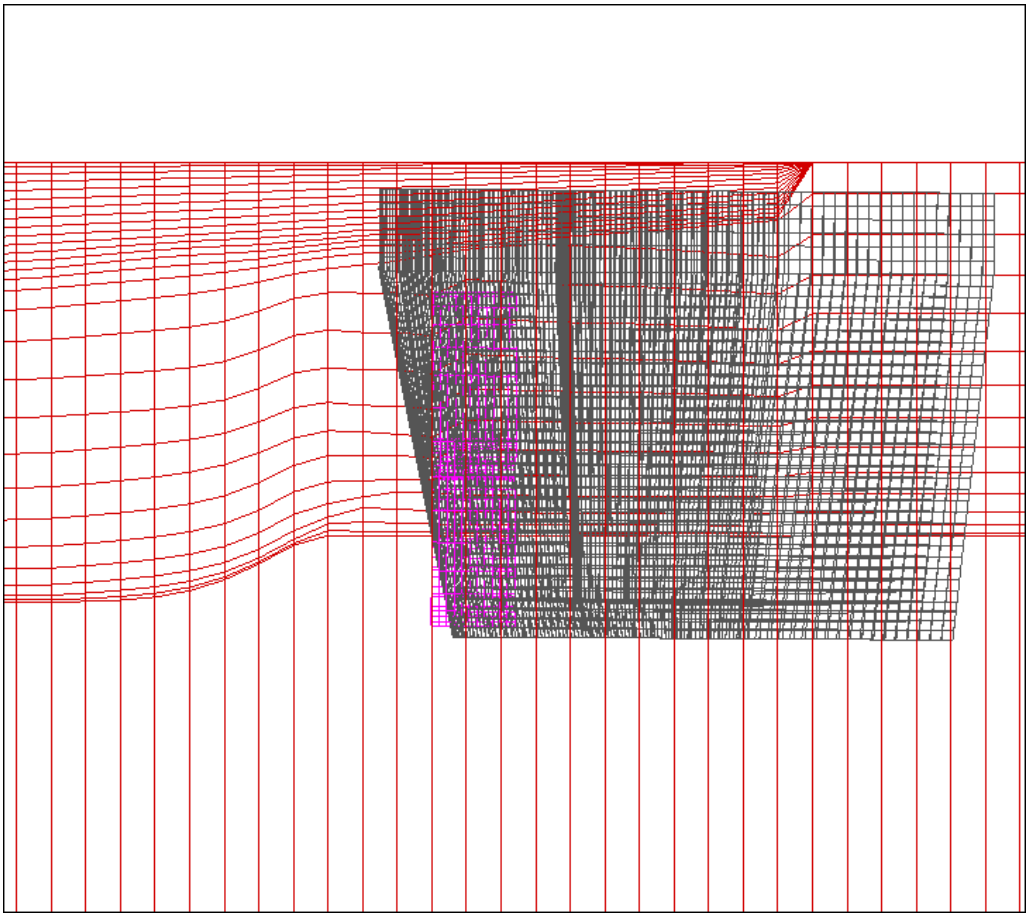

Figure 12. Overlapping grids

3.3. Work Procedure

In order to have a good comparison on computed results, computations have been done both in full scale and model scale.

Five different longitudinal locations of rudder in full scale and model scale have been investigated to come up with the best longitudinal position of the rudder. Also in model scale, for the optimum longitudinal position of rudder regarding the required delivered power, one altered transverse rudder position was also evaluated.

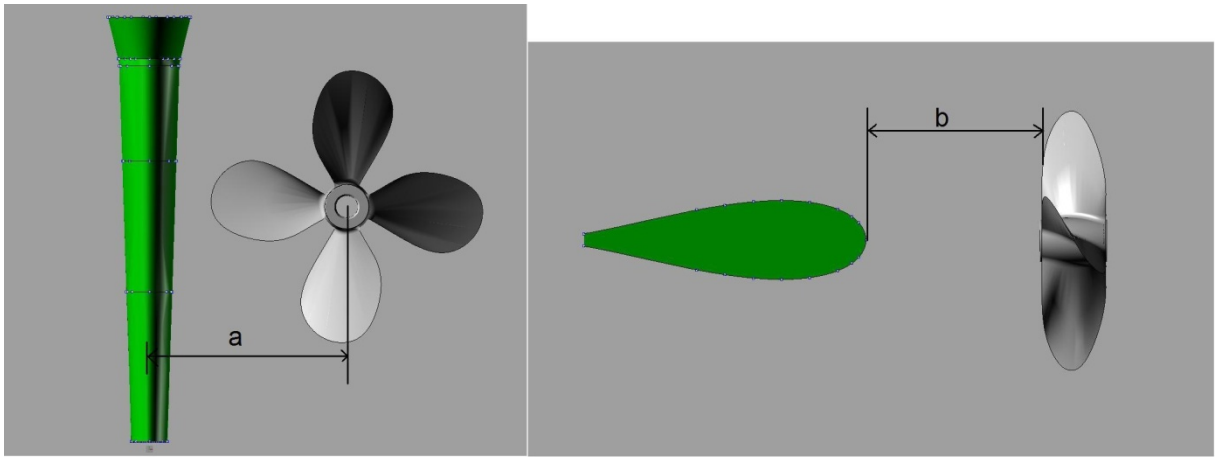

Figure 13. Definition of gap ratio and distance ratio

Some parameters, ratios and defined values regarding these parameters which were used in the computations are defined as:

- a/R = gap ratio, value used a/R = 0.1
- b/D = distance ratio, values used b/D = 0.24, 0.2, 0.17, 0.15, 0.1
- a = gap shown in Figure 13
- b = distance shown in Figure 13
- D = diameter of propeller
- R = radius of propeller

It should be mentioned that for full scale and model scale, self-propulsion test was applied for calculating the propeller characteristics. The reason for applying self-propulsion test is to adjust the J value to achieve the balance between thrust and drag. The wave drag which is computed by XPAN module is included in total drag. If the zonal approach is used for computing flow around the ship hull and propeller/rudder, which is the case for this project, then frictional drag computed by XBOUND for the fore body is also added to the total drag. The external tow force then is subtracted from the drag. The towing force is computed according to the ITTC78 procedure. CWTO which is the towing force coefficient should be calculated by equation 11 and imported as an input data into computation.

$$CTOW = CF_m - (CF_s + dCF_s) \tag{11}$$

$$CF_s = \frac{0.75}{(logR_{nL} - 2)^2} \tag{12}$$

$$CF_m = \frac{0.75}{(logR_{nL}-2)^2} \quad (13)$$

where CF_m and CF_s are the ITTC57 friction drag coefficients for model and ship respectively and dCF_s is a correction depending on the surface condition of the ship, which normally is dCF_s= 0.0004 [6].

Similar to the other computed forces by SHIPFLOW, nominal wetted area is used as a reference area to compute the tow force.

4. Comparison of the results

After running computations for five different longitudinal rudder positions from propeller in full scale and model scale and one transverse rudder position at a/R = 0.1 from propeller in model scale, results are compared to each other as diagrams and tables. At the first step, experimental results and predicted results are compared to calculated results for model scale and full scale respectively. At next step, for model scale and full scale, variation of thrust T, total resistance coefficient C_t and delivered power P_D in different rudder positions are investigated in order to determine the optimum rudder position. Flow fields of different positions are also compared to each other.

As it was mentioned before, for calculating propeller characteristics lifting line method is used which can be applied into the SHIPFLOW CFD computation by a command. During computations, advance ratio velocity J, i.e. RPM was being adjusted in order to achieve balance between thrust and drag which means that advance ratio velocity J varies during iterations. So delivered power P_D and thrust T are calculated with the J, i.e. RPM value corresponding to the K_q and K_t obtained from the last iteration results in CFD computations.

4.1. Comparison of experimental data with computed results in model scale

Experimental data for model scale was available regarding the self-propulsion test which has been performed on ship model with the scale factor of around α = 30. Ship model rudder position has been fixed in its original position during the tests, so there is no reported data from experiment for different rudder positions in this case. Therefore comparisons between experimental data and computed data were done regarding to the rudder position at b/D = 0.24 which is the original rudder position.

Table 3 shows some of the necessary results of computed self-propulsion test for ship model scale normalized by experimental values. By comparing the magnitude of obtained torque from computations and measured torque, it is seen that computed torque is around 1.4 % lower than the measured one. Also computed thrust is close to reported thrust from experiment which is 2.2 % lower than the measured one. The difference between computed bare hull resistance and measured bare hull resistance is higher compared to thrust and torque. In this case despite thrust and torque, computed resistance is around 13% higher than the measured one.

Table 3. Experimental data VS computed data for model scale at rudder position $\boldsymbol{b/D = 0.24}$

	Ship Speed V_s	Model Speed V_m	Torque Q	Thrust T	Resistance RTm	Rate of revs nm
Computed Data	1	1	0.986	0.978	1.135	1.032

Figure 14 shows axial velocity contours at propeller plane for ship model bare hull. Computed results which are in the left side illustrate an acceptable agreement with test results which are shown in the right side.
Consequently it is observed that computed results in model scale are very close to the reported data from the tests. Therefore it is concluded that computation results for model scale are reliable with a reasonable accuracy.

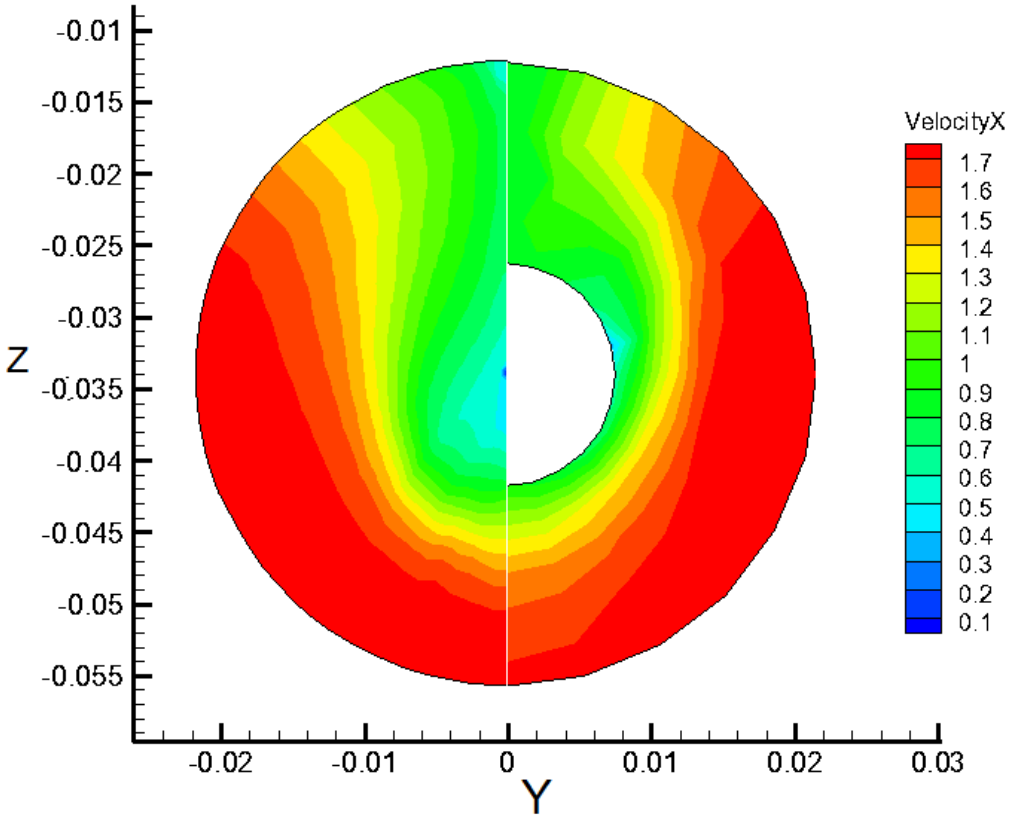

Figure 14. Velocity contours for bare hull at propeller plan, the calculated to left and the measured to the right

4.2. Comparison of predicted data with computed results in full scale

Table 4 presents some of the data obtained from CFD computations for full scale normalized by experimentally extrapolated data for full scale according to ITTC 1978 method and also similar.

Table 4. Predicted data according to ITTC1978 method VS computed data for full scale at rudder position $\mathbf{b/D = 0.24}$

	Ship Speed V_s	Effective power P_E	Delivered power P_D	Shaft rate ns	Torque Q	Thrust T	Total Efficiency
Computed Data	1	1.345	1.200	1.090	1.101	1.168	1.108

As seen computed data such as torque Q, thrust T, delivered power P_D and effective power P_E compared to predicted ones by ITTC 1978, are over predicted. While the computed K_q and K_t are rather close to predicted ones, over predicted values have been obtained because of low J value i.e. high RPM. The reason that can describe the low value of J is that the computed drag is too high. Ship hull grid resolution which is defined in XGRID module of SHIPFLOW is the same for model scale and full scale during computations which means in full scale probably the interpolation between the propeller grid and hull/rudder grids is inaccurate. The most common reason for this inaccuracy is that the hull grid is too coarse in the region where the

propeller grid is situated. So the interaction between hull and propeller will not be computed accurately. Therefore the results are not reliable.

As a rule of thumb there should be at least five cells in the XGRID mesh from the inlet and outlet of the propeller grid in this case it is 11 cells.

An improvement in the grid density of the ship hull was attempted in the region close to propeller by REFINE command which is used to change the grid locally. After several tries no appropriate results were achieved. Changing the grid density in XGRID is safer, but since the command file for computations in SHIPFLOW is the same for model scale and full scale, the only thing that can be changed is the grid stretching towards NOSLIP boundaries. The point is that, XGRID does not change the number of points in the normal direction, so increased stretching means that the grids get coarser. Furthermore, in discussion with Björn Regnström[1], he suggested to increase the ZETAMAX which is the number of panels in the radial direction by 10 to 15 which did not solve the problem in this case.

A grid study needs to be investigated to determine proper grid resolution at the aft part the ship hull. This task regarding to the lack of time can be done as future work.

4.3. Torque coefficient K_q/delivered power P_D in different rudder positions

Torque coefficient K_q is obtained as an output from CFD computations. It should be mentioned that in all computations in model scale, ship model speed is equal to what was used in the towing tank test, and in full scale, ship speed is equal to design conditions.

By moving the rudder towards the propeller, the trend of changing $K_q$in full scale and model scale as seen in Figure 15 is different. By looking at Figure 15, it is observed that in model scale by moving the rudder from its original position which is at b/D = 0.24 towards the propeller to b/D = 0.2, torque coefficient $K_q$was decreased. K_q Started to increase gradually after the rudder was proceeded from position b/D = 0.2 to b/D = 0.1.

In full scale, trend of changing K_q between b/D = 0.24 and b/D = 0.17 is the opposite of the model scale at the same positions. As it is seen in Figure 15, K_q was increased by moving the rudder between b/D = 0.24 and b/D = 0.2. But after it proceeded the position b/D = 0.2 to the b/D = 0.17, K_q was getting smaller with same rate as it was increasing between b/D = 0.24 and b/D = 0.2 .

Among all tested rudder positions for full scale, K_q gets the highest value at position b/D = 0.2. On the other hand lowest value of K_q is specified to the position b/D = 0.2 for model scale.

[1] Björn Regnström, developer of the overlapping grid RANS solver XCHAP at the company Flowtech International AB.

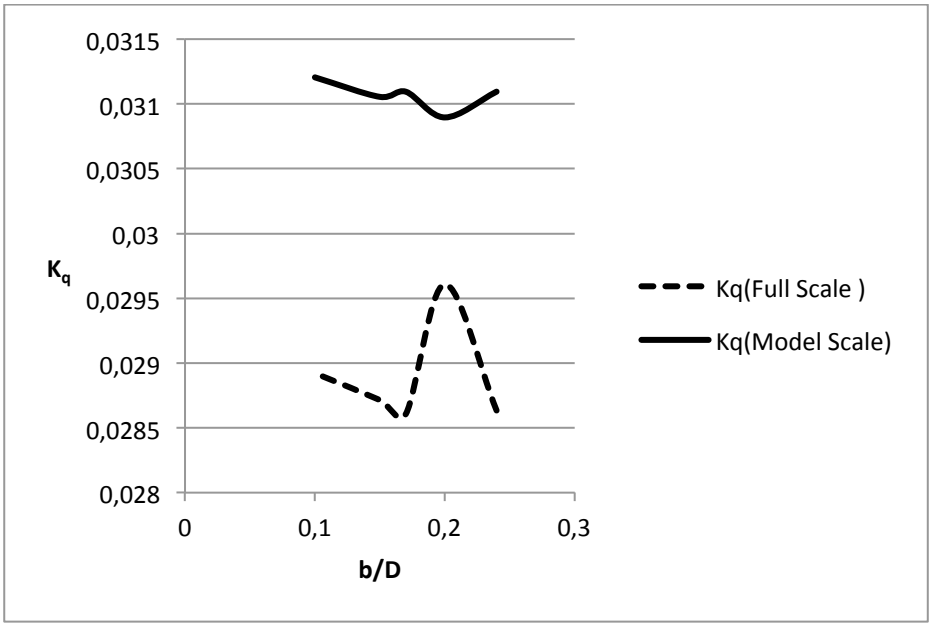

Figure 15. Computed K_q for full scale and model in different longitudinal rudder positions

Torque, Q, and delivered power to the shaft, P_D, are calculated according to equations 14 and 7. Results for Q and P_D in different rudder positions in full scale are shown in Table 5. Fluctuation of P_D at different rudder positions is shown in Figure 17. As it was mentioned before, advance ratio value J varies during iteration in order to make a balance between thrust and drag. Therefore, for different rudder positions, different values of J were obtained from CFD computations which affect the calculated torque Q and delivered power P_D.

As it is observed in Table 5, the highest value for J which means lowest RPM is allocated to position b/D = 0.1 . However K_q is not minimum at b/D = 0.1 but regarding to the equations 14 and 7, it is seen that the effect of RPM is two and three times more than K_q on the magnitude of torque Q and delivered power P_D respectively. So at position b/D = 0.1 lowest quantities for Q and P_D were obtained from calculations. Improvement of P_D at position b/D = 0.1 compare to original rudder position at b/D = 0.24 was 5.6 %. Location b/D = 0.2 is considered as a position among five different defined rudder positions which maximum power is delivered to the shaft to propel the ship with the speed of 20 knots. Calculated P_D at this point is around 4.43 % more than P_D of original position of rudder.

$$Q = 2\pi\rho n^2 D^5 K_q \tag{14}$$

Table 5. Computed data for full scale

b/D	J	K_q	Q [kN.m]	P_D [MW]
0.24	0.800642	0.0286366	1524.14	18.097
0.2	0.797677	0.0296086	1587.6	18.92
0.17	0.809642	0.0286072	1488.9	17.48
0.15	0.803064	0.0287147	1519.09	17.98
0.1	0.818986	0.0289217	1471.13	17.076

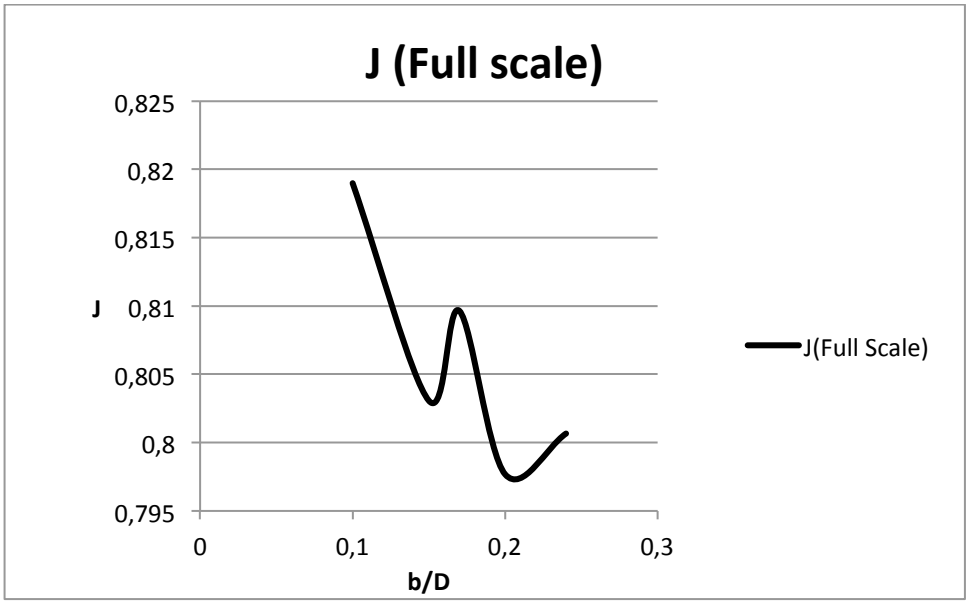

Figure 16. Variation of J at different rudder positions in full scale.

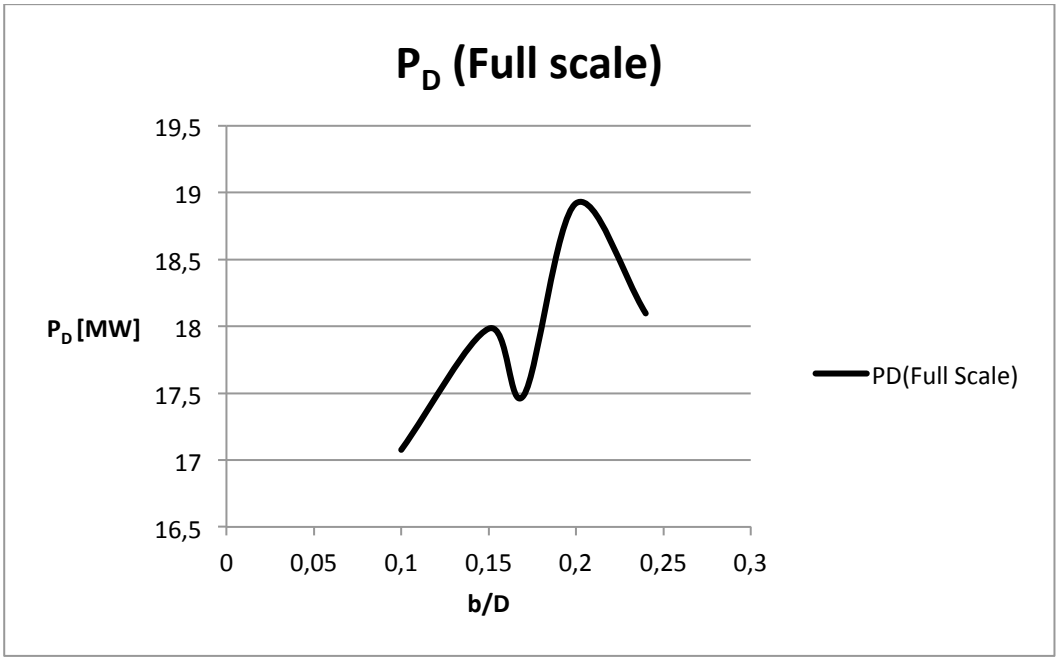

Figure 17. Variation of P_D at different rudder positions in full scale.

In model scale at position b/D = 0.2 as it is seen in Table 6 lowest value of Q and P_D has been calculated among five different longitudinal rudder positions. This happens regarding the lowest magnitude of K_q and highest advance velocity ratio J, i.e. lowest RPM which are allocated to this rudder position. Required delivered power P_D in this rudder position is around 6.3% less than computed P_D at original rudder position. The highest delivered power in model scale is allocated to the original rudder position at b/D = 0.24. Variation of J and P_D for model scale along the longitudinal direction between rudder and propeller are shown in Figure 18 and Figure 19 respectively.

Table 6. Computed data for model scale

b/D	J	K_q	Q [N.cm]	P_D [W]
0.24	0.845622	0.0310945	189.39	112.1
0.2	0.871167	0.0308964	177.31	104.94
0.17	0.853241	0.0310949	186.02	110.1
0.15	0.849705	0.0310552	187.33	110.87
0.1	0.854722	0.0312058	186.04	110.11

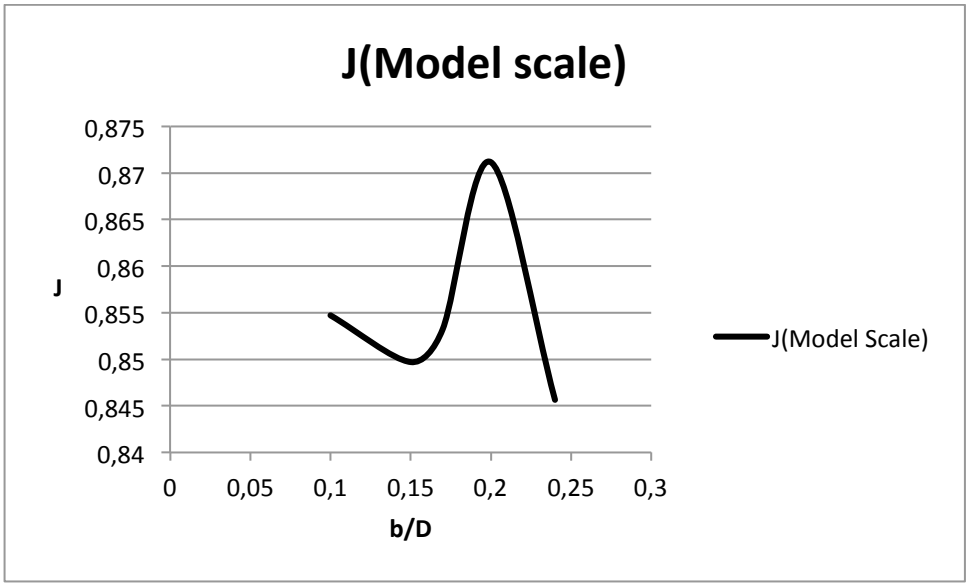

Figure 18. Variation of J at different rudder positions in model scale

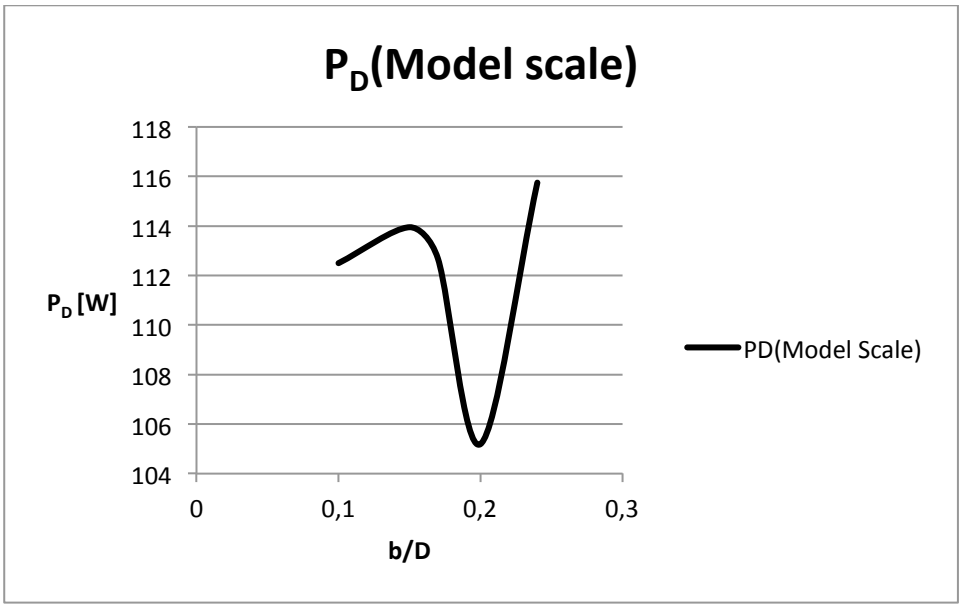

Figure 19. Variation of P_D at different rudder positions in model scale

4.3. Thrust coefficient K_t/thrust T in different rudder positions

K_t is also one of the other output results of SHIPFLOW computations for propeller which is called thrust coefficient. Computed results of K_t for model scale and full scale have been shown in Figure 20. By comparing Figure 15 with Figure 20, it is observed that the trend of fluctuation of K_t in model scale and full scale along the different rudder positions is similar to K_q fluctuation. In model scale highest value of K_t is allocated to the rudder position b/D = 0.1 while lowest K_t was calculated for rudder position b/D = 0.2. On the other hand in full scale, variation of $K_t$when the rudder is positioned at b/D = 0.2 is the opposite of the model scale which means, the highest value of K_t is obtained at this position. As it is seen in Table 7 and also in Figure 20 lowest value of K_t in full scale is allocated to rudder position b/D = 0.17 .

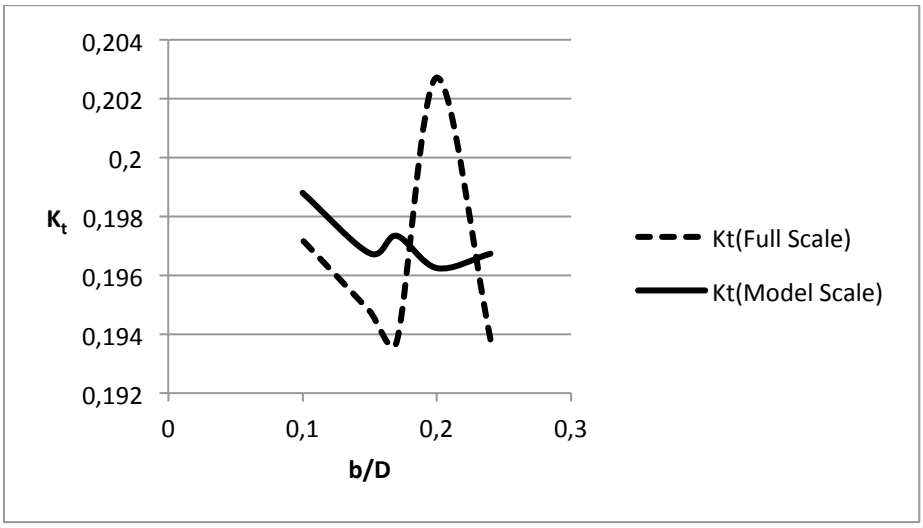

Figure 20. Computed K_t for full scale and model in different longitudinal rudder positions

Produced thrust by propeller is calculated according to equation 15. Regarding the tabulated data for full scale in Table 7 and drawn diagram in Figure 21, it is seen, at rudder position b/D = 0.2, J has the lowest value among five different rudder positions which means RPM is the highest , plus K_t has also the highest value in that location which ends up to give the highest magnitude for thrust T. Calculated thrust at this position is around 4.3 % more than calculated thrust at original rudder position.

$$T = K_t \rho n^2 D^4 \qquad (15)$$

Table 7. Calculated data for full scale

b/D	J	K_t	T [kN]
0.24	0.800642	0.193828	1277.245
0.2	0.797677	0.202719	1335.833
0.17	0.809642	0.193741	1276.671
0.15	0.803064	0.194783	1283.538
0.1	0.818986	0.197196	1299.438

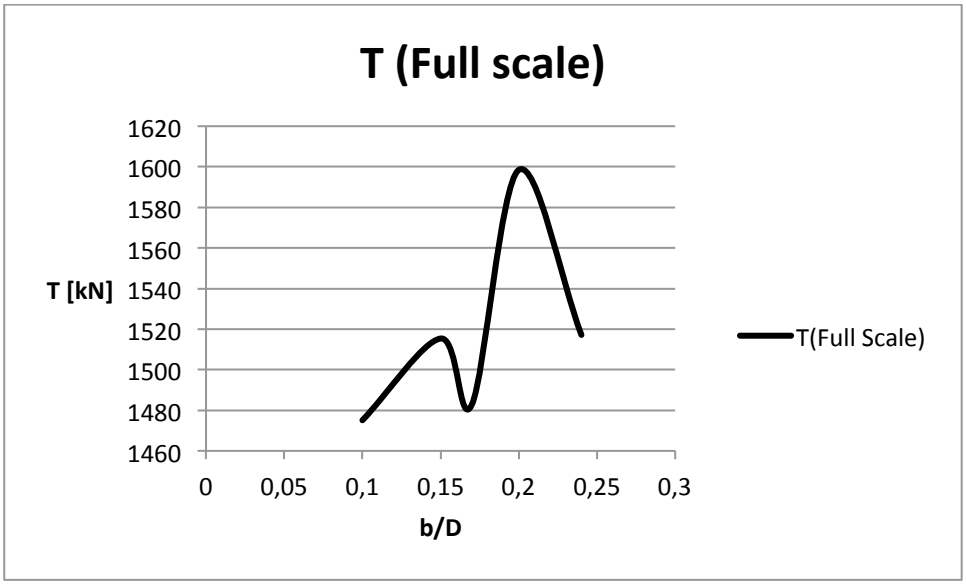

Figure 21. Variation of T at different rudder positions in full scale

In model scale by evaluating tabulated data in Table 8, it is observed that at the position b/D = 0.1, K_t has the highest value. On the other hand at position b/D = 0.24 which is the original position of the rudder J value is the lowest and therefore RPM is the highest among all tested positions. Consequently highest thrust is produced at b/D = 0.24 by the propeller. Lowest produced thrust is allocated to rudder position b/D = 0.2 which is around 6.5 % less than maximum produced thrust at b/D = 0.24.

Table 8. Calculated data for model scale

b/D	J	K_t	T [N]
0.24	0.845622	0.196733	52.1
0.2	0.871167	0.196247	48.96
0.17	0.853241	0.197345	51.33
0.15	0.849705	0.19675	51.6
0.1	0.854722	0.198804	51.53

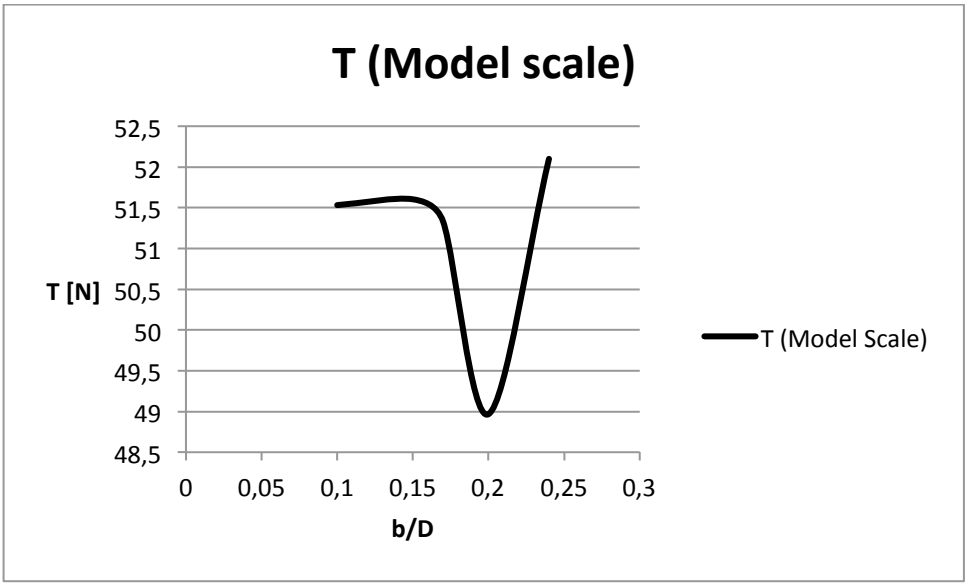

Figure 22. Variation of T at different rudder positions in model scale

4.4. Total resistance coefficient C_t in different rudder positions

For calculating total resistance coefficient C_t, wave resistance was also included into total resistance coefficient computations. As seen in Figure 23, C_t is changed when the rudder position varies in longitudinal direction. For comparing the total resistance coefficient C_t, in model scale and full scale, calculations were done for ship hull including propeller and appendages. Another calculation for obtaining total resistance coefficient in full scale was executed for ship hull which is including just appendages. As it is observed in Table 9, computed C_t in full scale for hull/propeller/appendages regarding to higher wetted surface area is higher than computed C_t for of hull/appendages. Resistance of naked ship hull and appendages which is calculated by equation 16, is used to calculate the effective power P_E [7].

$$R_{TS} = \frac{1}{2}\rho_s V_s^2 S_s C_{ts} \quad (16)$$

Table 9. Computed total resistance coefficient in full scale and model scale

b/D	C_t (Full Scale) Hull + Propeller + Append	C_t (Full Scale) Hull + Append	C_t (Model Scale) Hull + Propeller + Append
0.24	3.54E-03	3.13E-03	4.65E-03
0.2	3.35E-03	3.01E-03	4.47E-03
0.17	3.47E-03	3.07E-03	4.60E-03
0.15	3.53E-03	3.14E-03	4.62E-03
0.1	3.46E-03	3.06E-03	4.60E-03

According to Figure 23 which shows the trend of variation of computed C_t for model scale and full scale along the different rudder positions, it is observed that in model scale and full scale,C_t is decreased when rudder is moved from original location to b/D = 0.2 . After the rudder is passed from b/D = 0.2, C_t begins to increase. In model scale between positions b/D = 0.17 and b/D = 0.1, resistance coefficient C_t almost stays constant. Fluctuation of C_t in both cases of full scale as it is seen in Figure 23 after position b/D = 0.17 has sharper negative slope in comparison with model scale. Minimum value for total resistance coefficient C_t is obtained at position b/D = 0.2 in both full scale and model scale. The trend of C_t

fluctuation agrees with the trend of thrust T fluctuation in model scale but in full scale the trends of thrust T and total resistance coefficient C_t variation are completely different with each other. For example at position b/D = 0.2 produced thrust is maximum which is in conflict with the minimum total resistance coefficient at this position.

This contrast between thrust and total resistance coefficients will be discussed in discussion part of this report.

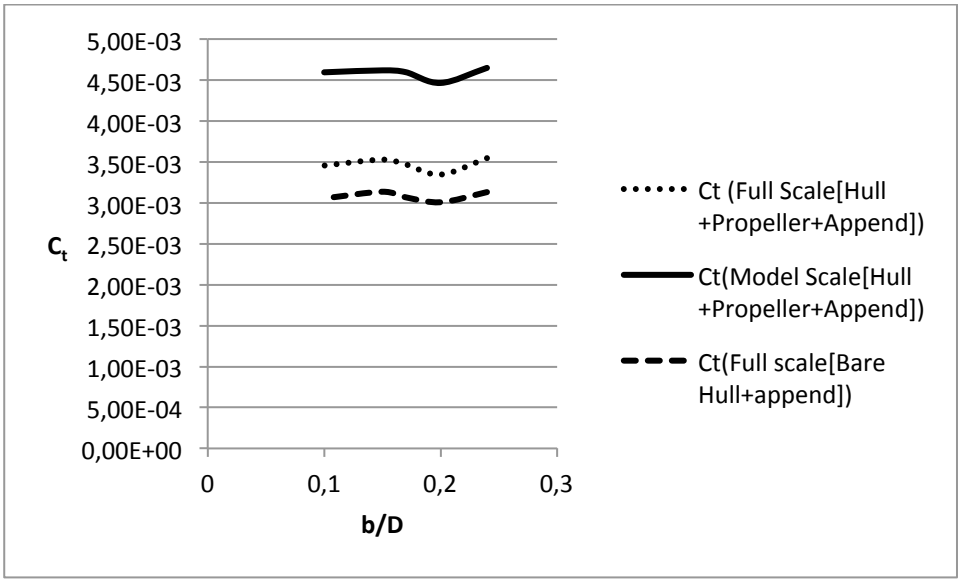

Figure 23. Variation of total resistance coefficient C_t in full scale and model scale

4.5. Computed results for two different transverse rudder positions

Regarding the experimental research that has been done by K.KAFALI [4] at MIT University about evaluating the effect of different rudder positions on propeller characteristics, it was observed that for twin screw ship, between transverse rudder positions a/R = 0.1 to a/R = 0.2, propeller characteristics are optimum.

In this study, investigation is carried out on a single screw ship. However, in reality for single screw ships, rudder is positioned in the shaft line direction, but it is interesting to see the effect of moving the rudder transversely on the propeller operation. In model scale at optimum longitudinal rudder position at b/D = 0.2, position a/R = 0.1 as an altered transverse position was chosen to be investigated and compared to the original transverse rudder position (a/R = 0) at the same longitudinal position b/D = 0.2.

As it is shown in Table 10, at transverse rudder position a/R = 0.1, improvement in all tabulated parameters related to this transverse positions is observed. For example delivered power P_D has been improved around 37% which is not logical and makes these obtained values at a/R = 0.1 questionable regarding their accuracy. One idea about these strange improvements can be referred to inaccurate interpolation between overlapped grids. More study needs to be done in the case of moving the rudder in transverse direction in order to investigate how it will affect the required delivered power and also the manoeuvrability of the ship.

Table 10. Comparison between two different transverse positions

a/R	K_q	K_t	Shaft rate ns [1/s]	Torque Q [N.cm]	Thrust T [N]	Delivered power P_D [W]	C_t
0	0.0308	0.19624	9.44	177.3	48.96	105.19	0.004465
0.1	0.0275	0.16792	8.4	125.1	33.15	66.03	0.00435

4.6. Flow field

In order to study the effect of different rudder positions on the flow around the rudder, axial velocity contours were computed and investigated for model scale, for four different positions along the rudder. As it is shown in Figure 24, they are located at leading edge, middle of the rudder, trailing edge and behind the trailing edge.

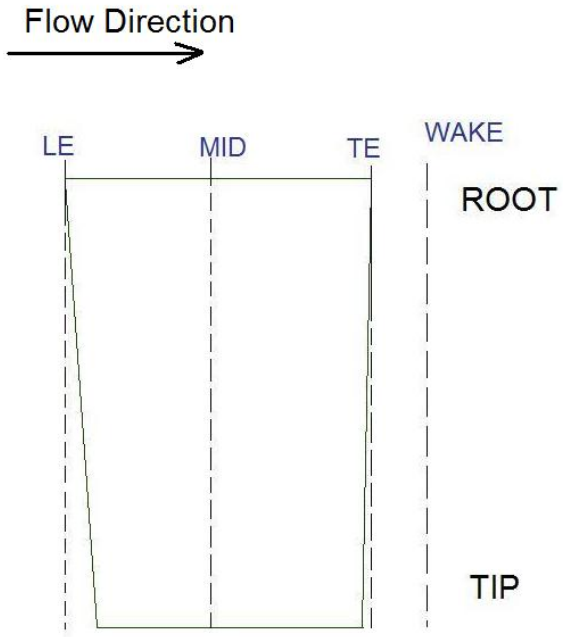

Figure 24. Four different positions along the rudder

The results of computed axial velocity contours for model scale are shown in Figure 25 to Figure 30. By moving the rudder step by step from its original location towards the propeller, it is seen that at leading edge of the rudder, at both starboard and port side of the rudder, high velocity region becomes larger till rudder approached to position $b/D = 0.17$. After position $b/D = 0.17$ it again becomes smaller until position $b/D = 0.1$. Furthermore it can be mentioned that at leading edge, flow is more accelerated in pressure side of the rudder which is in the starboard side compared to suction side.

At middle of the rudder as it is observed in Figure 25 to Figure 30 for all rudder positions, vortex at the tip was developing.

At farther downstream stations such as trailing edge and behind the trailing, more development in rudder tip vortex took place regarding the pressure difference between pressure side and suction side. This pressure difference with associating of rotation of the

flow, created high-velocity area on the starboard side which directed the flow to move downwards around the tip and in the port side helped the flow to move upwards to the root.

Boundary layer was developing step by step from leading edge to trailing edge. On the starboard side maximum growth of boundary layer is observed at middle of the rudder. On the other hand on port side, maximum development of boundary later is seen at the trailing edge of the rudder.

At the position behind the trailing edge as it is seen in Figure 25 to Figure 29, low-velocity area for the rudder position $b/D = 0.1$ which is the closest rudder position, is larger compared to other longitudinal rudder positions from propeller.

Figure 30 shows velocity contours of rudder for different positions along the rudder at rudder longitudinal position $b/D = 0.2$ and transverse position $a/R = 0.1$. As it is seen, low-velocity areas in this rudder position are larger and rounder compared to other shown velocity contours of different rudder positions. Also high-velocity areas which mostly located close to rudder surface on the portside of the rudder are smaller than other shown velocity contours.

In the right side of the Figure 25 to Figure 30 cross flow vectors are shown. At the middle of the propeller, cross flow shows rotation of the slipstreams near the rudder tip which points to developing the tip vortex at this position. At the farther positions along the rudder, more development in tip vortex is observed which regarding to this tip vortex, at the pressure side of the rudder, cross flow vectors were conducted downward and on the suction side, they were conducted upwards. At the middle of the rudder, at the upper part of the suction side, as it is seen in Figure 25 to Figure 30, direction of cross flow just before reaching to the rudder surface is perpendicular to the rudder surface. Then regarding the rudder blockage effect, some of the cross flow vectors were directed upwards and some of them downwards. Similar behaviour to some extent is observed in the lower part of the pressure side. At the position behind trailing edge where there is no blocking of the rotational slipstreams, effect of the rudder on the flow is still observed.

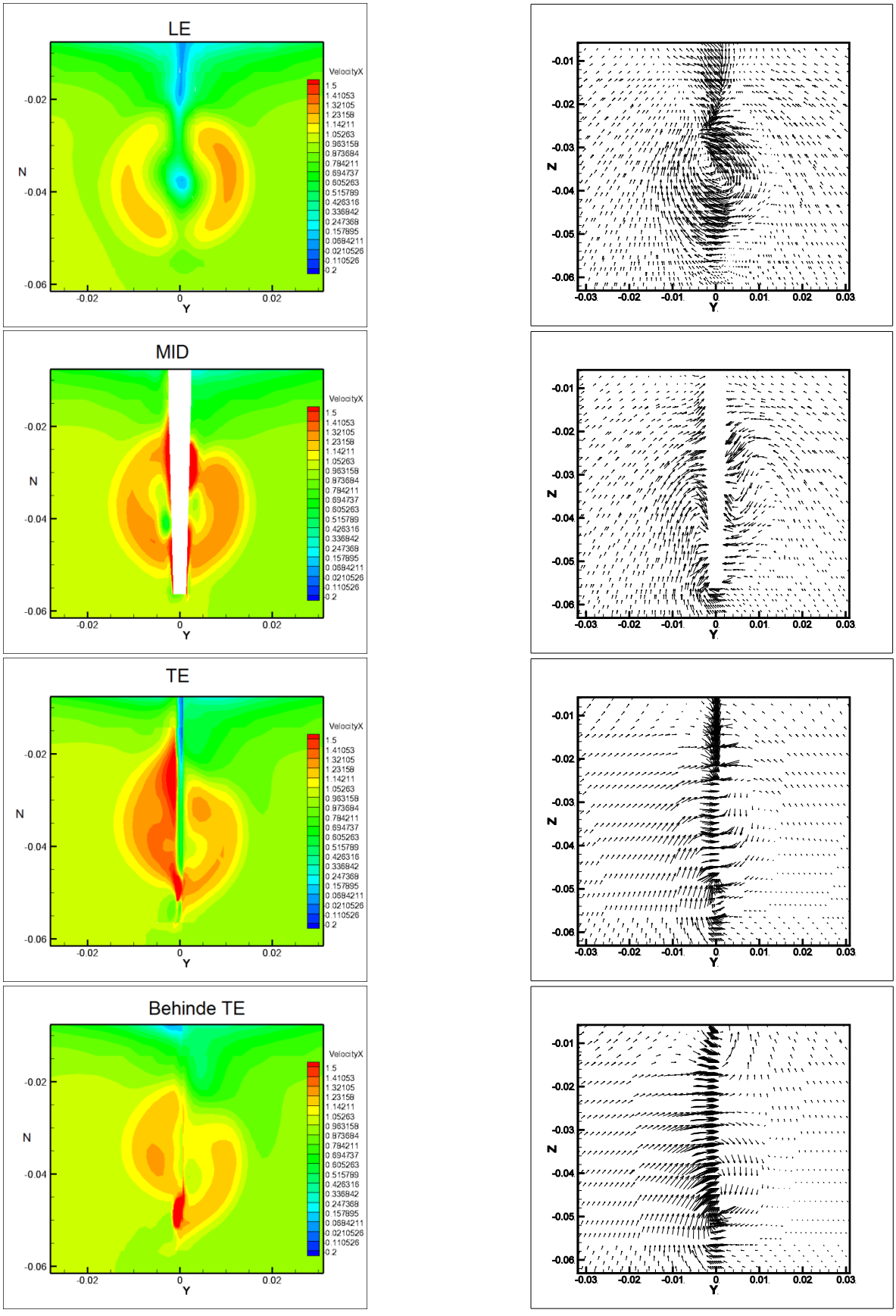

Figure 25. Axial velocity contours and cross flow vectors across along the rudder at model scale related to rudder position $\mathbf{b/D = 0.24}$

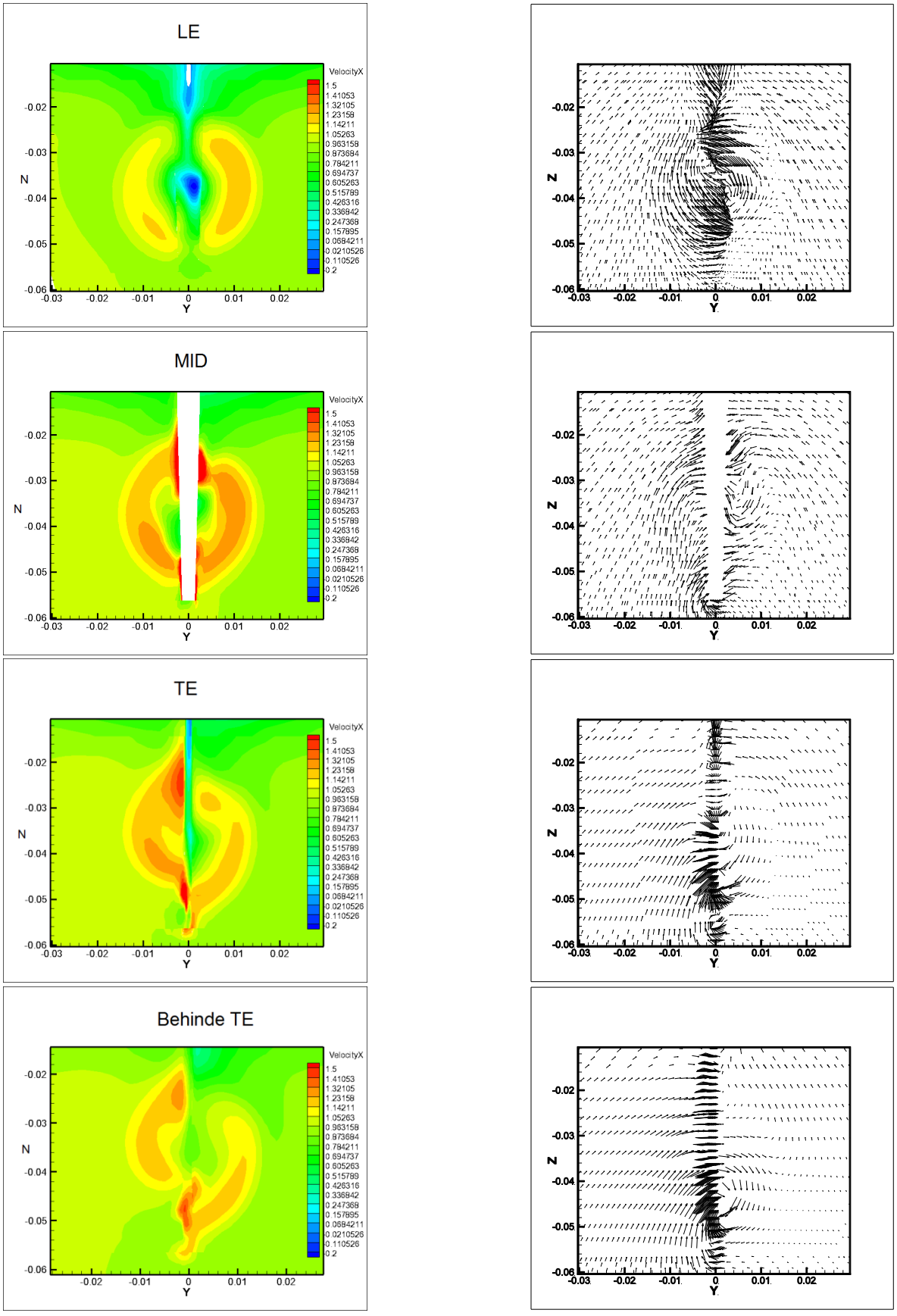

Figure 26. Axial velocity contours and cross flow vectors across along the rudder at model scale related to rudder position $\mathbf{b/D = 0.2}$

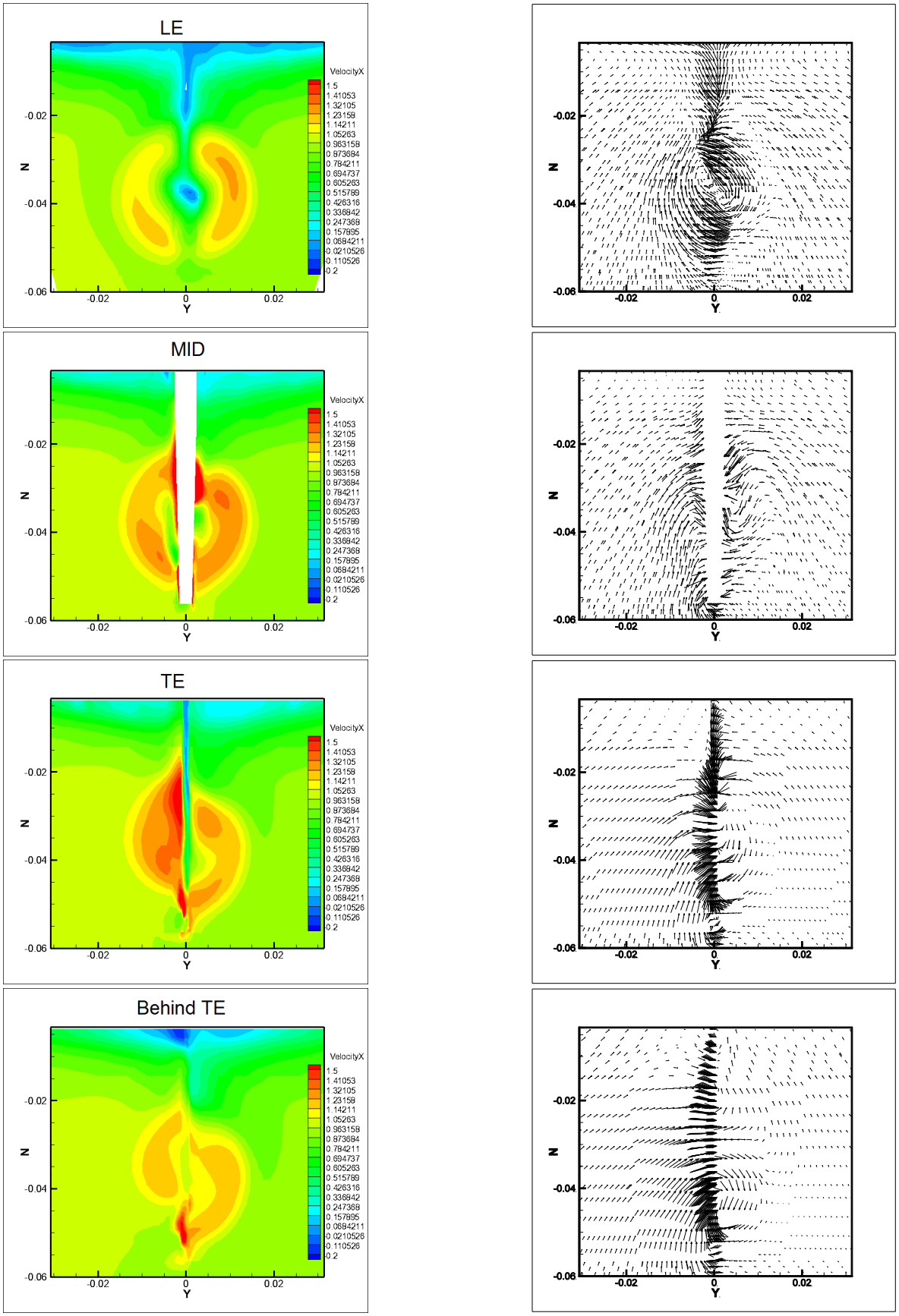

Figure 27. Axial velocity contours and cross flow vectors across along the rudder at model scale related to rudder position $\mathbf{b/D = 0.17}$

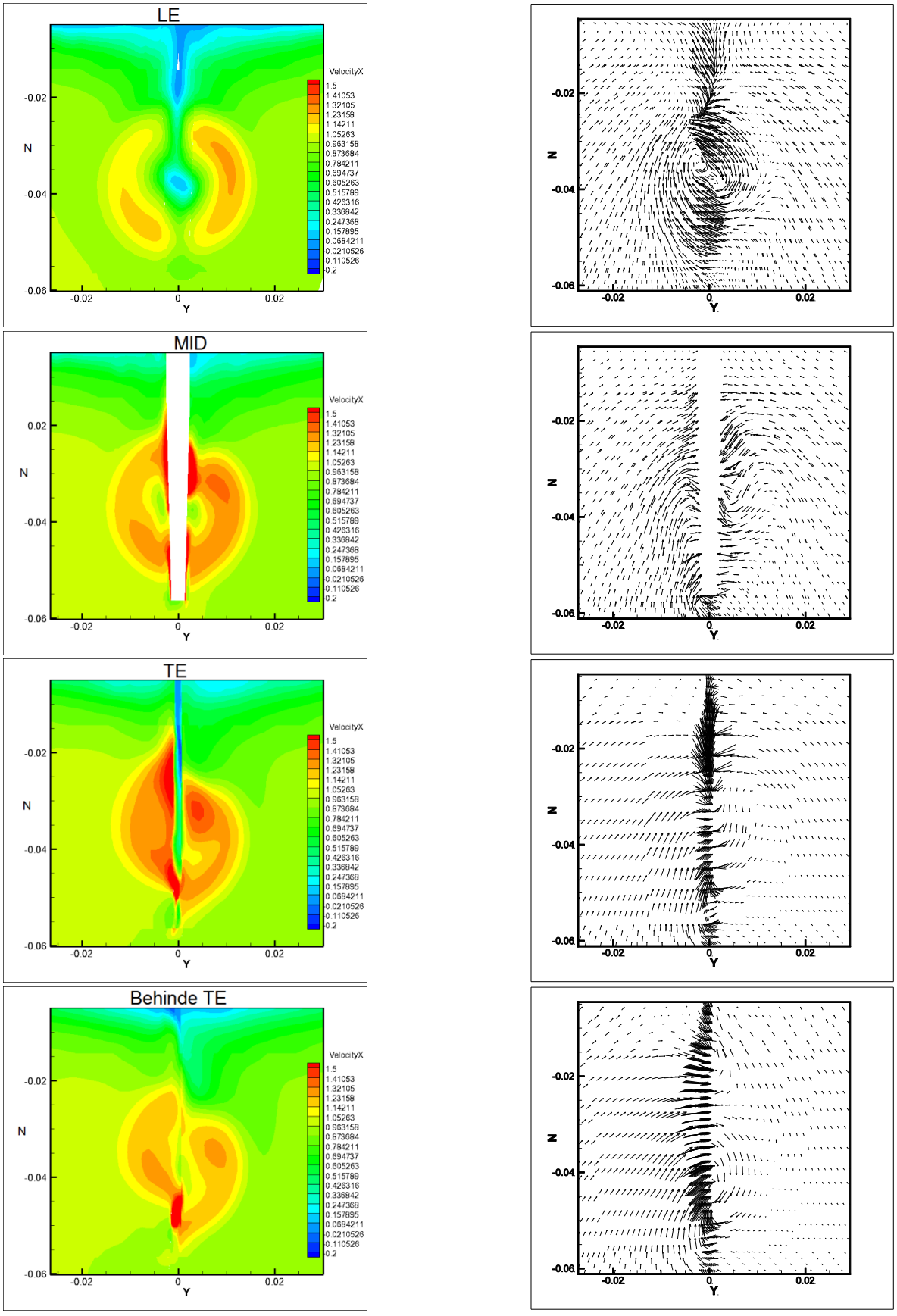

Figure 28. Axial velocity contours and cross flow vectors across along the rudder at model scale related to rudder position $\mathbf{b/D = 0.15}$

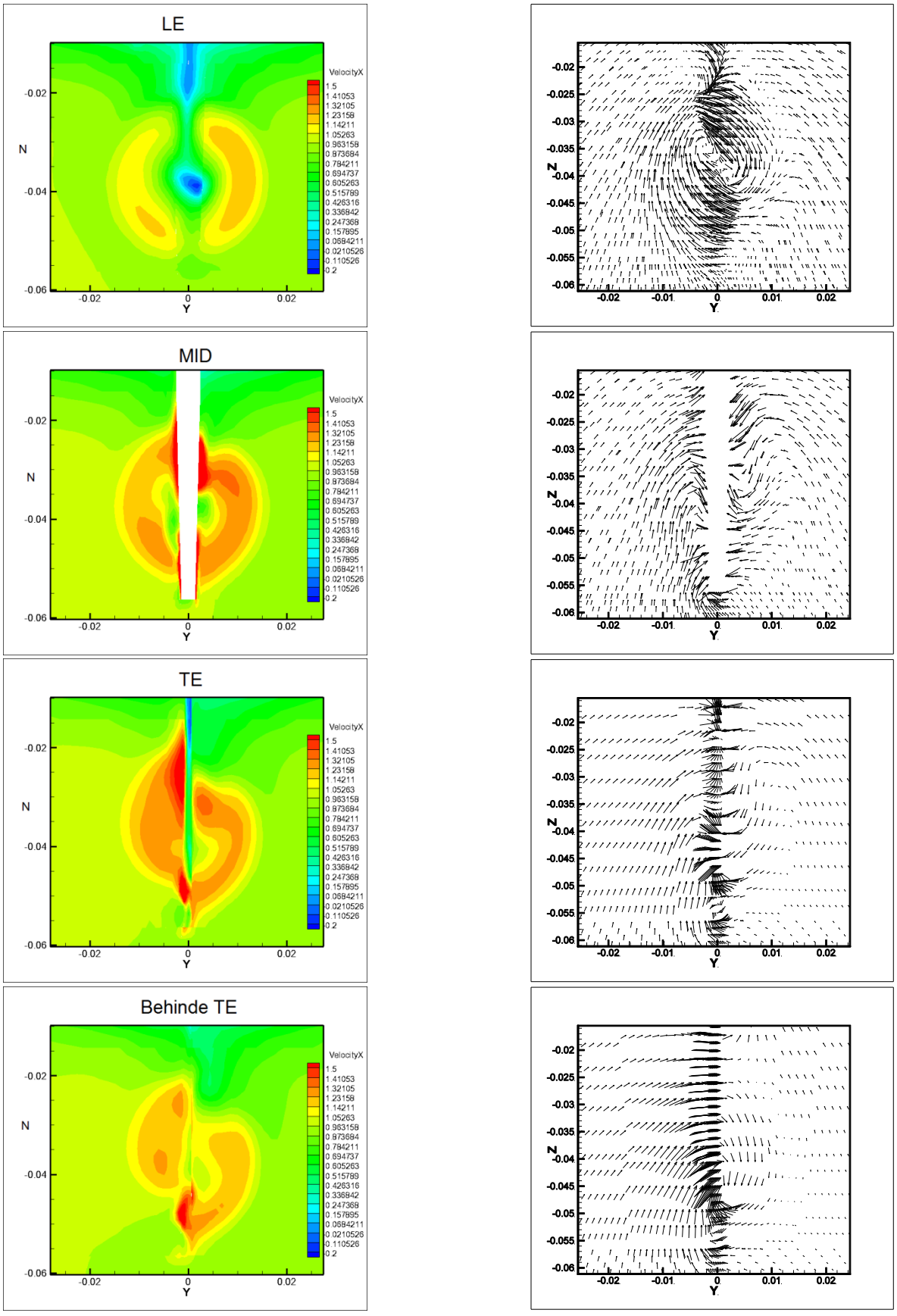

Figure 29. Axial velocity contours and cross flow vectors across along the rudder at model scale related to rudder position $\mathbf{b/D = 0.1}$

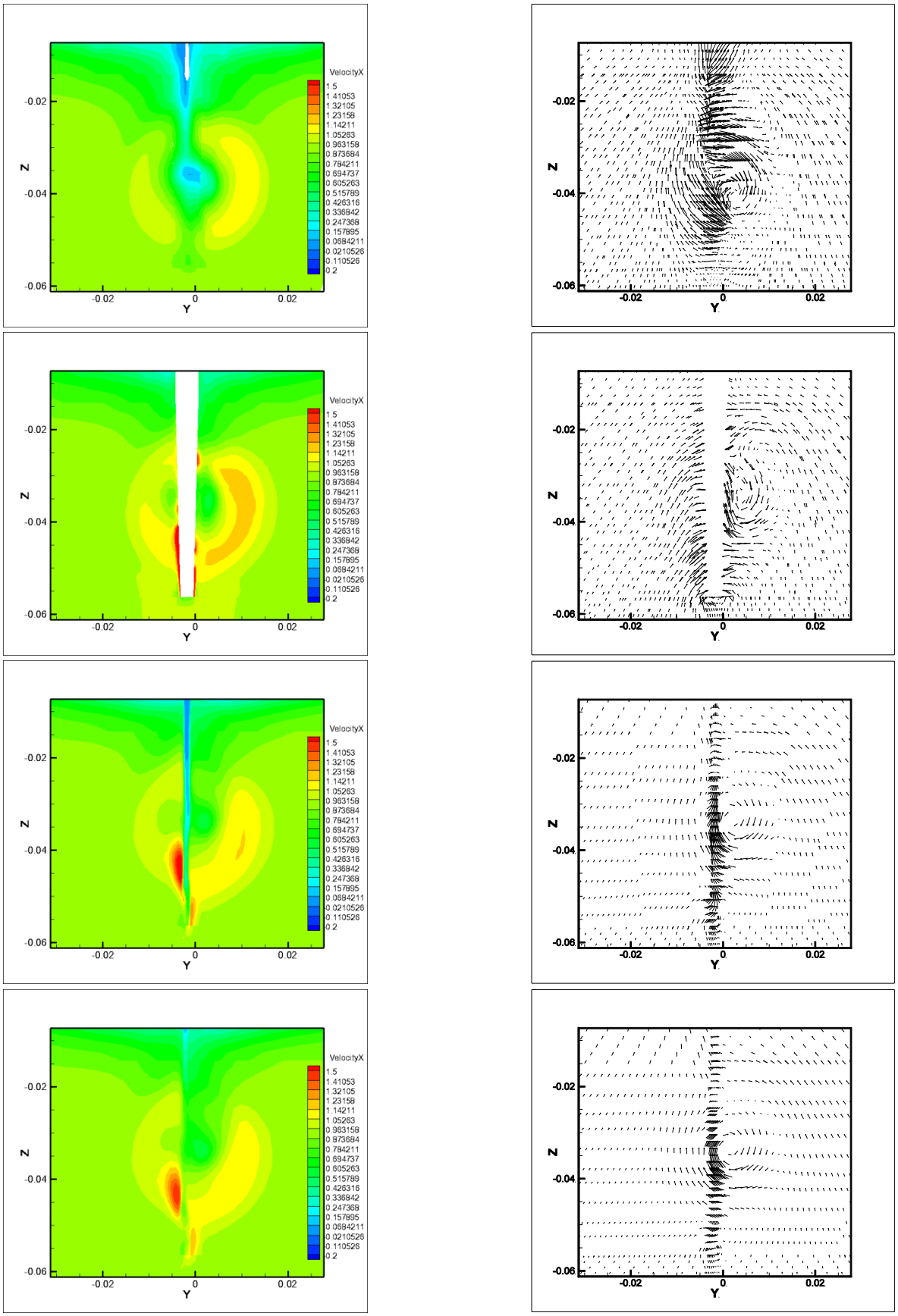

Figure 30. Axial velocity contours and cross flow vectors across along the rudder at model scale related to rudder positions $\mathbf{b/D = 0.2}$ and $\mathbf{a/R = 0.1}$

4.7. Pressure distribution on rudder surface

The pressure distribution on the surface of the rudder for different rudder positions is shown in Figure 31 to Figure 36. The images in the left side represent the pressure side of the rudder and the right images show the suction side of the rudder for all rudder positions.

The effect of the propeller to induce different pressure distribution on the both sides of the rudder is totally obvious from the figures. At the leading edge, two high and low pressure regions can be seen in the both sides of the rudder. The high pressure regions are located at the lower part of pressure side and at the upper part of suction side which are as a result of hitting the spin of the slipstreams to these areas. The shadow effect of the rudder has created two low-pressure areas at the leading edge which are located at the same spanwise as the high-pressure regions.

The low pressure region at the pressure side is located above the high-pressure area while at suction side it is below the region of high pressure. Further along the rudder and just behind the aforementioned high and low pressures regions, another low pressure zone has been observed which are located at the leading edge. It may be argued that the accelerated flow in the slipstream is a reason for the creation of this low pressure area. It is also important to note that at the pressure side, this low pressure area is expanded to the tip of the rudder. At the suction side of the rudder, almost close to the tip, a high pressure region is also formed which is expected because of the tip vortex caused by the pressure difference between two sides of the rudder and can be easily seen in the velocity contour plots. As it is observed in Figure 35, among the different rudder positions, the largest high pressure area near the trailing edge is observed for the rudder with b/D = 0.1. This happens, because probably more swirl slipstreams hit this area at this specific position.

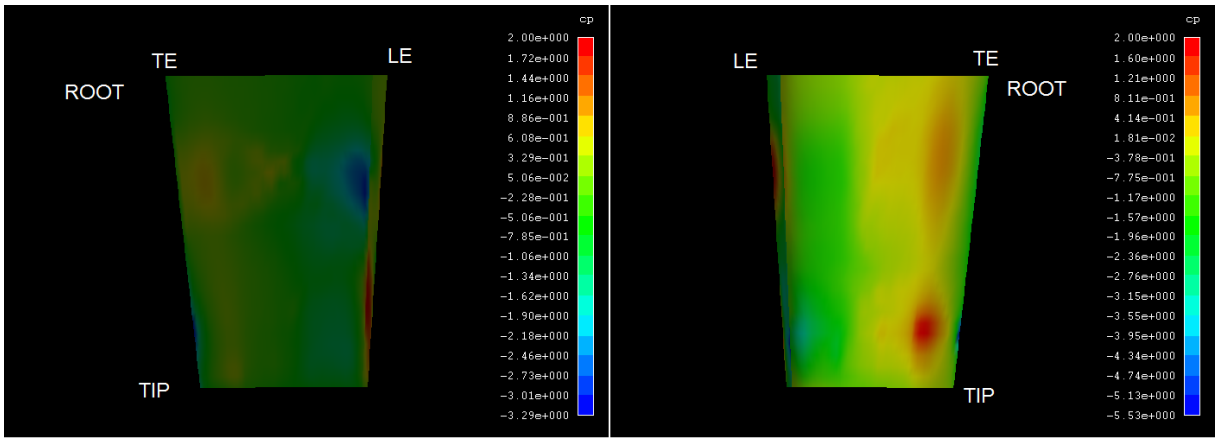

Figure 31. Pressure distribution on pressure side (left image) and suction side (right image) of the rudder at position $\mathbf{b/D = 0.24}$

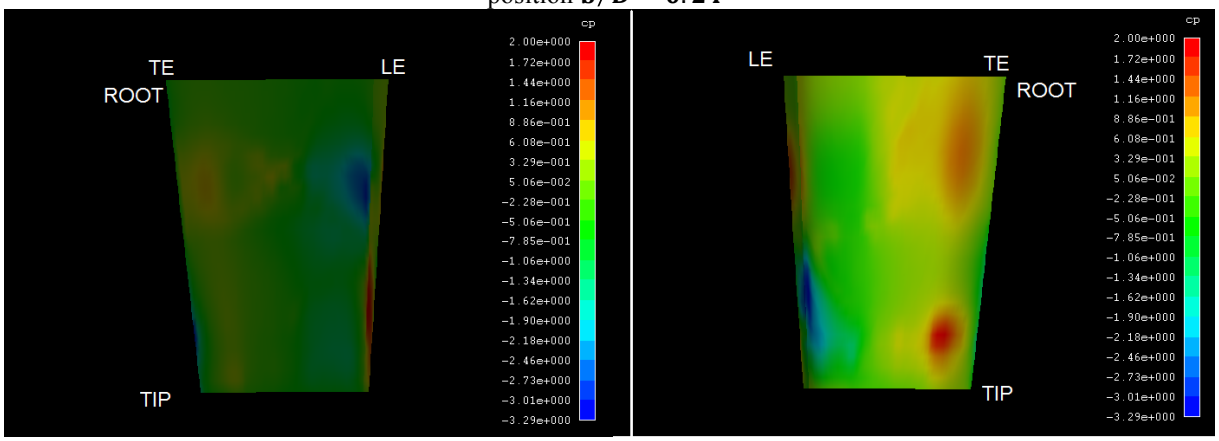

Figure 32. Pressure distribution on pressure side (left image) and suction side (right image) of the rudder at position $\mathbf{b/D = 0.2}$

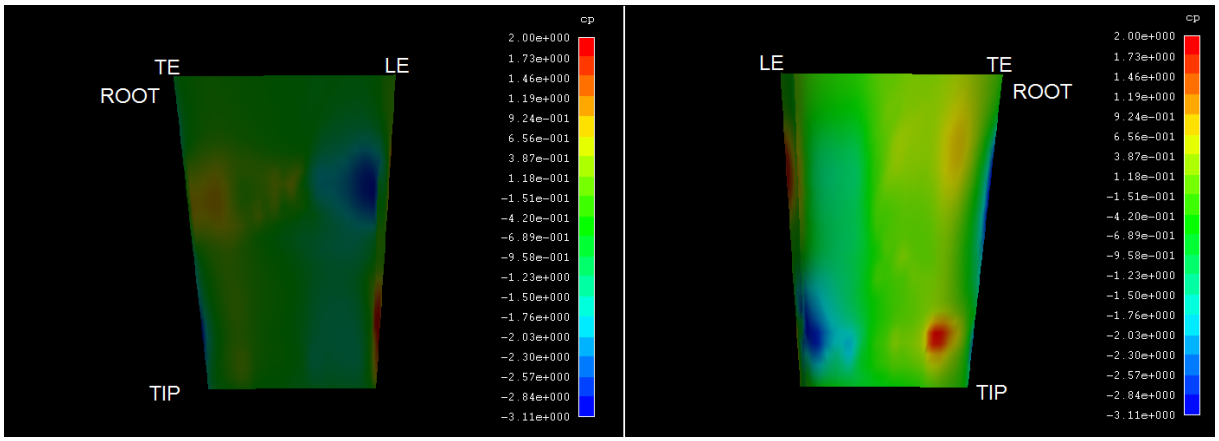

Figure 33. Pressure distribution on pressure side (left image) and suction side (right image) of the rudder at position $\mathbf{b/D = 0.17}$

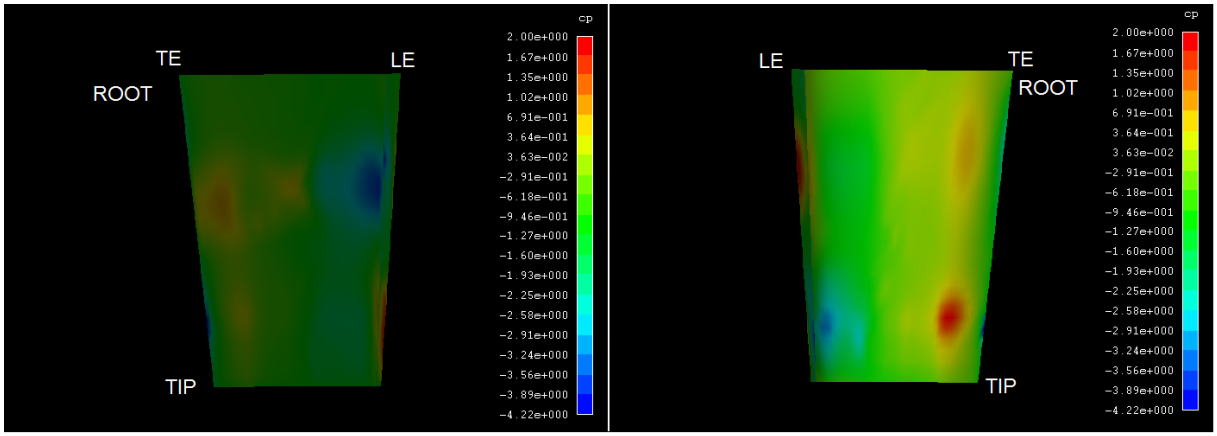

Figure 34. Pressure distribution on pressure side (left image) and suction side (right image) of the rudder at position $\mathbf{b/D = 0.15}$

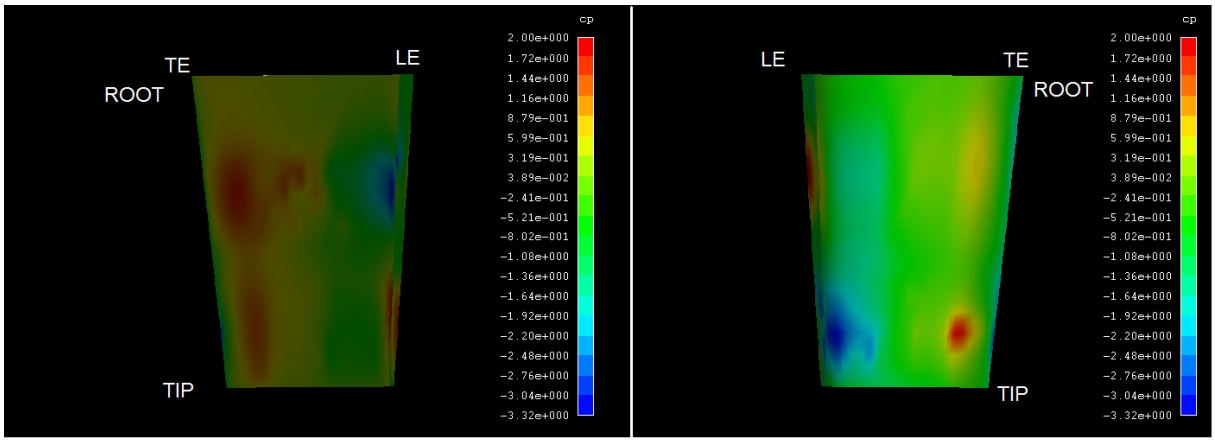

Figure 35. Pressure distribution on pressure side (left image) and suction side (right image) of the rudder at position $\mathbf{b/D = 0.1}$

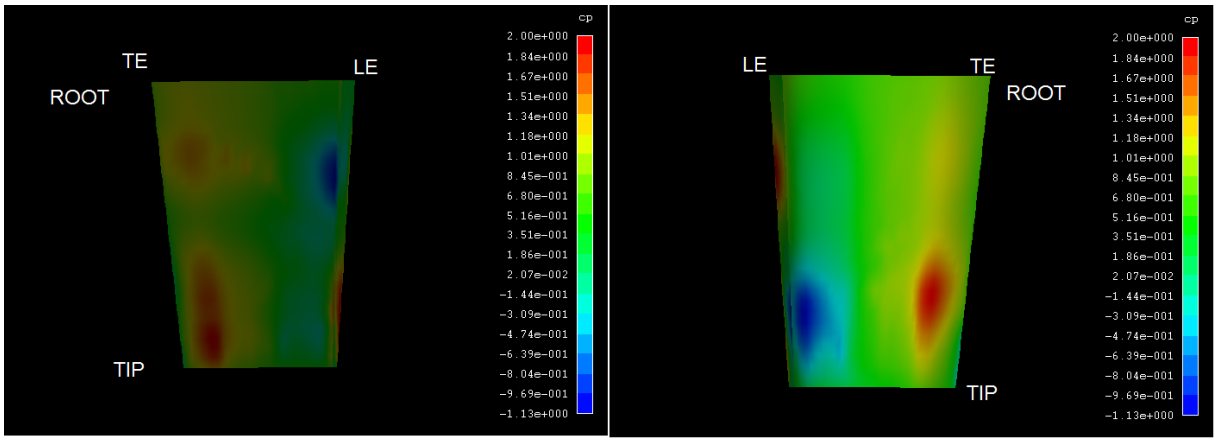

Figure 36. Pressure distribution on pressure side (left image) and suction side (right image) of the rudder at positions $\mathbf{b/D = 0.2}$ and $\mathbf{a/R = 0.1}$

5. Discussion and conclusions

Regarding to varying the rudder position in order to determine less required delivered power to propel the ship in a specific speed for model scale and corresponding of that speed in full scale, two different rudder positions were determined based on computation results. For model scale, optimum rudder location regarding to delivered power was determined at b/D = 0.2, while in full scale it was determined at b/D = 0.1. Different optimum rudder positions in model scale and full scale are doubtful. Other questionable results can be referred to computed total resistance coefficient for full scale. As it was seen in Figure 17, Figure 21 and Figure 23, fluctuation of total resistance coefficient C_t for full scale does not agree with the fluctuation of torque and thrust. For example at position b/D = 0.2, C_t is minimum, where the magnitudes of torque Q and thrust T are expected to be minimum as well, but they are not. While C_t fluctuation in different rudder positions in model scale completely agrees with torque and thrust fluctuations.

By comparing the results obtained from computations for full scale with predicted results calculated based on reliable ITTC1978 method, it was observed that computed results are not reasonable and over predicted in comparison with predicted results by ITTC1978 method. As it was mentioned before, one possibility which can describe these unreasonable computed results for full scale is inaccurate interpolation between propeller grids and coarse grids of the aft part of the hull. The flow characteristics regarding the hull/propeller interaction will not be computed accurately which also affects the computed results of interaction between propeller/ rudder and flow parameters around the rudder.

Computed results for model scale which showed a good agreement with experimental results, is satisfactory with a reasonable accuracy. However if the variations of P_D, T and J for different rudder positions in model scale were smoother, the reliability of results would be higher. According to Table 6 and Table 9, at longitudinal rudder position b/D = 0.2, total resistance of the ship hull including propeller and appendages is minimum and consequently, calculated delivered power P_D for this rudder position is minimum as well among five investigated longitudinal rudder positions. However the results for delivered power were improved when the located rudder at b/D = 0.2 was moved transversely to a different transverse positions at a/R = 0.1, but the improvement does not seem logical and needs more investigation and study.

According to all calculations which have been done for full scale and model scale, it is concluded that without considering the loss in manoeuvrability, if the design limitations permit, from propulsion characteristics point of view, optimum longitudinal position for rudder in model scale, located at distance ratio b/D = 0.2 .

6. Future work

There are several tasks in this thesis which are interesting to be done as future work in order to make some of the results more accurate and reliable.

- A grid study needs to be done on full scale in order to find the appropriate grid resolution in ship hull in order to have an accurate interpolation between propeller grids and hull grids.
- Investigating several gap ratios for those five distance ratios in order to come up with the best location of rudder according to propulsion characteristics point of view
- Several types of rudders can be examined in order to evaluate how the rudder geometry can affected the optimum rudder position.
- As it is known, manoeuvrability which is an important parameter will be considered in determining the optimum rudder position. In order to determine which rudder position is used, an investigation needs to be done to evaluate how much manoeuvrability will be lost or gained for different rudder positions.
- Cavitation is also interesting to be considered for different evaluated rudder positions.

7. References

[1] Bark, G. and Dyne, G., 2005, Ship propulsion MMA 155, Department of Shipping and Marine Technology, Chalmers University of Technology, Göteborg.

[2] Da-Qing Li, 1994, Investigation on Propeller-Rudder Interaction by numerical Methods, Department of Shipping and Marine Technology, Chalmers University of Technology, Göteborg.

[3] SHIPFLOW 4.3 Users Manual, 2010, Flowtech International AB, Göteborg.

[4] K.KAFALI, 1961, Propeller characteristics with different locations of the rudders in the propeller race of twin rudders-twin screws ships, Journal of the American Society for Naval Engineers, Vol.73, Issue 2, pp. 369–376, May 1961

[5] KAI-JIA HAN, 2008, Numerical optimization of hull/propeller/rudder configurations, Department of Shipping and Marine Technology, Chalmers University of Technology, Göteborg.

[6] Larsson, L. and Raven, H. C., 2004, MMA 155 Ship Resistance and Flow, Göteborg and Wageningen, Chalmers University of Technology.

[7] K. J. Rawson, E. C. Tupper, 2001, Basic Ship Theory, vol.2, 5th ed, p. 385.

[8] www.manbw.com/files/news/filesof3859/P254-04-04.pdf

8. Appendix

Sample of computations command file for model scale

```
xflow
  title     ( titl="The HTC, Lifting Line Propeller" )
  program   ( all )
  hulltype ( mono,h1gr="hull", ogrp="stern",
             fbgr="bulb", abgr="boss",fsflow,transom )
  offsetfile( file="shipflow_wallenious_offset.shf", xaxdir=-1.0, ysign=1.0,
             xori=190, zori=10, lpp=190 )
  ipos      ( trim = 0.41 )
  vship     ( fn=[0.22], rn=[13.6e6] )
  prop      (id="ID0",xsh=3.78,zsh=3.56,dprop=6.8,dhub=1.02,
       nbla=4, jv=0.825, ear=0.591, numb=10,
        r_rt=[0.2,0.3,0.4,0.5,0.6,0.7,0.8,0.9,0.95,1],
        p_d =[0.7128,0.795,0.8716,0.9375,0.9815,0.9893,0.9459,0.8391,0.7593,0.6615]
thic=[0.2813,0.2377,0.1973,0.1601,0.126,0.0951,0.0674,0.0428,0.0318,0],
leng=[1.4374,1.6331,1.8332,2.020,2.1652,2.2326,2.1866,1.8506,1.3948,0],
camb=[0.0365,0.0466,0.0508,0.051,0.0491,0.046,0.0404,0.0317,0.0243,0],
rotdir = 1 )
symm      ( nosy )
end
xpan
 cont( free, nonlinear )
 iter( maxit = 20 )
 twcut( on )
end
 xgrid
  size ( ksimax=120,etamax=30,zetamax=60)
  xdistr ( xstart = 0.5, ksi1 =40 ,ksi2 =85,
  xch1 = 0.85, xch2=1.05, xend=1.5 )

end

xchap

   import (id="001", file="extended.fmt" ,
   number=1 , scale=1,TRANSLATION=[-0.45,0,0] )
                import (id="002", file="extended.fmt" ,
                number=2 , scale=1,TRANSLATION=[-0.45,0,0] )
                import (id="003", file="extended.fmt" ,
                number=3 , scale=1,TRANSLATION=[-0.45,0,0] )
                import (id="004", file="extended.fmt" ,
                number=4 , scale=1,TRANSLATION=[-0.45,0,0] )
                import (id="005", file="extended.fmt" ,
                number=5 , scale=1,TRANSLATION=[-0.45,0,0] )
```

```
                import (id="006", file="extended.fmt" ,
                number=6 , scale=1,TRANSLATION=[-0.45,0,0] )
                import (id="007", file="extended.fmt" ,
                number=7 , scale=1, bc32 ="noslip",TRANSLATION=[-0.45,0,0] )
                import (id="008", file="extended.fmt" ,
                number=8 , scale=1,TRANSLATION=[-0.45,0,0] )
                import (id="009", file="extended.fmt" ,
                number=9 , scale=1, bc12 ="slip",TRANSLATION=[-0.45,0,0] )
                import (id="010", file="extended.fmt" ,
                number=10 , scale=1, bc32 ="noslip",TRANSLATION=[-0.45,0,0] )
                import (id="011", file="extended.fmt" ,
                number=11 , scale=1, bc31 ="noslip",TRANSLATION=[-0.45,0,0] )
                import (id="012", file="extended.fmt" ,
                number=12 , scale=1,TRANSLATION=[-0.45,0,0] )
                import (id="013", file="extended.fmt" ,
                number=13 , scale=1, bc31 ="noslip",TRANSLATION=[-0.45,0,0] )
                import (id="014", file="extended.fmt" ,
                number=14 , scale=1,TRANSLATION=[-0.45,0,0] )
                import (id="015", file="extended.fmt" ,
                number=15 , scale=1, bc12 ="slip",TRANSLATION=[-0.45,0,0] )
                import (id="016", file="extended.fmt" ,
                number=16 , scale=1,TRANSLATION=[-0.45,0,0] )
                import (id="017", file="extended.fmt" ,
                number=17 , scale=1, bc22 ="noslip",TRANSLATION=[-0.45,0,0] )
                import (id="018", file="extended.fmt" ,
                number=18 , scale=1, bc21 ="noslip",TRANSLATION=[-0.45,0,0] )
                import (id="019", file="extended.fmt" ,
                number=19 , scale=1, bc11 ="noslip",TRANSLATION=[-0.45,0,0] )
                parallel( nthread=2 )
   lline  (on, id="ID0",self, CTOW =1.054e-3, cf=0.0054)
                control (start, maxi =2000, nostret  )
end
```

Sample of XCHAP solver out-put file for model scale

```
- MAXIMUM TOTAL WAKE VARIATION, PROPELLER: ID0
  WVAR ( maximum total wake variation )       :  0.479832
  WRAD ( maximum found at radius )            :  1.000000

 - MEAN WAKE FRACTION, PROPELLER: ID0
   Wn = 0.0619523


 - COEFFICIENTS, PROPELLER: ID0
   Kt = 0.196733
   Kq = 0.0310945
   Jv = 0.845622

 - IMPO

   id   = 001
   file  = extended.fmt
   grou  = 1
   stre  = 1
   cut   = 1
   scal  = 1
   ysig  = -1
   trim  = 1
   rota  = (0,0,0)
   rotc  = (0,0,0)
   tran  = (-0.45,0,0)
   bc11  = "INTERIOR"
   bc12  = "INTERIOR"
   bc21  = "INTERIOR"
   bc22  = "INTERIOR"
   bc31  = "INTERIOR"
   bc32  = "INTERIOR"
   numb  = 1

 - IMPO

   id   = 002
   file  = extended.fmt
   grou  = 1
   stre  = 1
   cut   = 1
   scal  = 1
   ysig  = -1
   trim  = 1
   rota  = (0,0,0)
   rotc  = (0,0,0)
```

```
  tran  =  (-0.45,0,0)
  bc11  =  "INTERIOR"
  bc12  =  "INTERIOR"
  bc21  =  "INTERIOR"
  bc22  =  "INTERIOR"
  bc31  =  "INTERIOR"
  bc32  =  "INTERIOR"
  numb  =  2

- IMPO

  id    =  003
  file  =  extended.fmt
  grou  =  1
  stre  =  1
  cut   =  1
  scal  =  1
  ysig  =  -1
  trim  =  1
  rota  =  (0,0,0)
  rotc  =  (0,0,0)
  tran  =  (-0.45,0,0)
  bc11  =  "INTERIOR"
  bc12  =  "INTERIOR"
  bc21  =  "INTERIOR"
  bc22  =  "INTERIOR"
  bc31  =  "INTERIOR"
  bc32  =  "INTERIOR"
  numb  =  3

- IMPO

  id    =  004
  file  =  extended.fmt
  grou  =  1
  stre  =  1
  cut   =  1
  scal  =  1
  ysig  =  -1
  trim  =  1
  rota  =  (0,0,0)
  rotc  =  (0,0,0)
  tran  =  (-0.45,0,0)
  bc11  =  "INTERIOR"
  bc12  =  "INTERIOR"
  bc21  =  "INTERIOR"
  bc22  =  "INTERIOR"
  bc31  =  "INTERIOR"
  bc32  =  "INTERIOR"
  numb  =  4
```

```
- IMPO

  id   = 005
  file = extended.fmt
  grou = 1
  stre = 1
  cut  = 1
  scal = 1
  ysig = -1
  trim = 1
  rota = (0,0,0)
  rotc = (0,0,0)
  tran = (-0.45,0,0)
  bc11 = "INTERIOR"
  bc12 = "INTERIOR"
  bc21 = "INTERIOR"
  bc22 = "INTERIOR"
  bc31 = "INTERIOR"
  bc32 = "INTERIOR"
  numb = 5

- IMPO

  id   = 006
  file = extended.fmt
  grou = 1
  stre = 1
  cut  = 1
  scal = 1
  ysig = -1
  trim = 1
  rota = (0,0,0)
  rotc = (0,0,0)
  tran = (-0.45,0,0)
  bc11 = "INTERIOR"
  bc12 = "INTERIOR"
  bc21 = "INTERIOR"
  bc22 = "INTERIOR"
  bc31 = "INTERIOR"
  bc32 = "INTERIOR"
  numb = 6

- IMPO

  id   = 007
  file = extended.fmt
  grou = 1
  stre = 1
  cut  = 1
```

```
  scal = 1
  ysig = -1
  trim = 1
  rota = (0,0,0)
  rotc = (0,0,0)
  tran = (-0.45,0,0)
  bc11 = "INTERIOR"
  bc12 = "INTERIOR"
  bc21 = "INTERIOR"
  bc22 = "INTERIOR"
  bc31 = "INTERIOR"
  bc32 = "NOSLIP"
  numb = 7

- IMPO

  id   = 008
  file = extended.fmt
  grou = 1
  stre = 1
  cut  = 1
  scal = 1
  ysig = -1
  trim = 1
  rota = (0,0,0)
  rotc = (0,0,0)
  tran = (-0.45,0,0)
  bc11 = "INTERIOR"
  bc12 = "INTERIOR"
  bc21 = "INTERIOR"
  bc22 = "INTERIOR"
  bc31 = "INTERIOR"
  bc32 = "INTERIOR"
  numb = 8

- IMPO

  id   = 009
  file = extended.fmt
  grou = 1
  stre = 1
  cut  = 1
  scal = 1
  ysig = -1
  trim = 1
  rota = (0,0,0)
  rotc = (0,0,0)
  tran = (-0.45,0,0)
  bc11 = "INTERIOR"
  bc12 = "SLIP"
```

```
  bc21 = "INTERIOR"
  bc22 = "INTERIOR"
  bc31 = "INTERIOR"
  bc32 = "INTERIOR"
  numb = 9

- IMPO

  id   = 010
  file = extended.fmt
  grou = 1
  stre = 1
  cut  = 1
  scal = 1
  ysig = -1
  trim = 1
  rota = (0,0,0)
  rotc = (0,0,0)
  tran = (-0.45,0,0)
  bc11 = "INTERIOR"
  bc12 = "INTERIOR"
  bc21 = "INTERIOR"
  bc22 = "INTERIOR"
  bc31 = "INTERIOR"
  bc32 = "NOSLIP"
  numb = 10

- IMPO

  id   = 011
  file = extended.fmt
  grou = 1
  stre = 1
  cut  = 1
  scal = 1
  ysig = -1
  trim = 1
  rota = (0,0,0)
  rotc = (0,0,0)
  tran = (-0.45,0,0)
  bc11 = "INTERIOR"
  bc12 = "INTERIOR"
  bc21 = "INTERIOR"
  bc22 = "INTERIOR"
  bc31 = "NOSLIP"
  bc32 = "INTERIOR"
  numb = 11

- IMPO
```

```
  id   = 012
  file = extended.fmt
  grou = 1
  stre = 1
  cut  = 1
  scal = 1
  ysig = -1
  trim = 1
  rota = (0,0,0)
  rotc = (0,0,0)
  tran = (-0.45,0,0)
  bc11 = "INTERIOR"
  bc12 = "INTERIOR"
  bc21 = "INTERIOR"
  bc22 = "INTERIOR"
  bc31 = "INTERIOR"
  bc32 = "INTERIOR"
  numb = 12

- IMPO

  id   = 013
  file = extended.fmt
  grou = 1
  stre = 1
  cut  = 1
  scal = 1
  ysig = -1
  trim = 1
  rota = (0,0,0)
  rotc = (0,0,0)
  tran = (-0.45,0,0)
  bc11 = "INTERIOR"
  bc12 = "INTERIOR"
  bc21 = "INTERIOR"
  bc22 = "INTERIOR"
  bc31 = "NOSLIP"
  bc32 = "INTERIOR"
  numb = 13

- IMPO

  id   = 014
  file = extended.fmt
  grou = 1
  stre = 1
  cut  = 1
  scal = 1
  ysig = -1
  trim = 1
```

```
  rota = (0,0,0)
  rotc = (0,0,0)
  tran = (-0.45,0,0)
  bc11 = "INTERIOR"
  bc12 = "INTERIOR"
  bc21 = "INTERIOR"
  bc22 = "INTERIOR"
  bc31 = "INTERIOR"
  bc32 = "INTERIOR"
  numb = 14

- IMPO

  id   = 015
  file = extended.fmt
  grou = 1
  stre = 1
  cut  = 1
  scal = 1
  ysig = -1
  trim = 1
  rota = (0,0,0)
  rotc = (0,0,0)
  tran = (-0.45,0,0)
  bc11 = "INTERIOR"
  bc12 = "SLIP"
  bc21 = "INTERIOR"
  bc22 = "INTERIOR"
  bc31 = "INTERIOR"
  bc32 = "INTERIOR"
  numb = 15

- IMPO

  id   = 016
  file = extended.fmt
  grou = 1
  stre = 1
  cut  = 1
  scal = 1
  ysig = -1
  trim = 1
  rota = (0,0,0)
  rotc = (0,0,0)
  tran = (-0.45,0,0)
  bc11 = "INTERIOR"
  bc12 = "INTERIOR"
  bc21 = "INTERIOR"
  bc22 = "INTERIOR"
  bc31 = "INTERIOR"
```

```
  bc32 = "INTERIOR"
  numb = 16

- IMPO

  id   = 017
  file = extended.fmt
  grou = 1
  stre = 1
  cut  = 1
  scal = 1
  ysig = -1
  trim = 1
  rota = (0,0,0)
  rotc = (0,0,0)
  tran = (-0.45,0,0)
  bc11 = "INTERIOR"
  bc12 = "INTERIOR"
  bc21 = "INTERIOR"
  bc22 = "NOSLIP"
  bc31 = "INTERIOR"
  bc32 = "INTERIOR"
  numb = 17

- IMPO

  id   = 018
  file = extended.fmt
  grou = 1
  stre = 1
  cut  = 1
  scal = 1
  ysig = -1
  trim = 1
  rota = (0,0,0)
  rotc = (0,0,0)
  tran = (-0.45,0,0)
  bc11 = "INTERIOR"
  bc12 = "INTERIOR"
  bc21 = "NOSLIP"
  bc22 = "INTERIOR"
  bc31 = "INTERIOR"
  bc32 = "INTERIOR"
  numb = 18

- IMPO

  id   = 019
  file = extended.fmt
  grou = 1
```

```
 stre  =  1
 cut   =  1
 scal  =  1
 ysig  =  -1
 trim  =  1
 rota  =  (0,0,0)
 rotc  =  (0,0,0)
 tran  =  (-0.45,0,0)
 bc11  =  "NOSLIP"
 bc12  =  "INTERIOR"
 bc21  =  "INTERIOR"
 bc22  =  "INTERIOR"
 bc31  =  "INTERIOR"
 bc32  =  "INTERIOR"
 numb  =  19

 OVERLAPPING GRID SECTION

No of frames             : 21
No of grids              : 21
No of points             : 666168
No of interpolation cells : 181971
No of discretization cells: 639467
No of outside cells      : 19624
Total no of cells        : 841062

 Standard deviation for forces in XCHAP
 (Displayed in percent of average force)
 std(CPV)=                          :   0.07 %
 std(CF)=                           :   0.00 %

- Resistance:

 CF    ( Frictional resist. coeff. )        : 2.527E-03
 CPV   ( Viscous pres. resist. coeff. )     : 1.373E-03
 CV    ( Viscous resist. coeff. )           : 3.900E-03
 CW    ( Wave resist. coeff. )              : 7.467E-04
 CT    ( Total resist. coeff. )             : 4.646E-03
 K     ( Form factor )                      : 0.370
 S     ( Wetted surface / L**2 )            : 0.240

SHIPFLOW exited: 2010-10-12 at  18:20:23 total cpu-time =  171380.635 s
```